



Available online at www.sciencedirect.com

ScienceDirect

Geochimica et Cosmochimica Acta 166 (2015) 327–343

Geochimica et  
Cosmochimica  
Acta

www.elsevier.com/locate/gca

# A revised Pitzer model for low-temperature soluble salt assemblages at the Phoenix site, Mars

J.D. Toner <sup>a,\*</sup>, D.C. Catling <sup>a</sup>, B. Light <sup>b</sup>

<sup>a</sup> University of Washington, Box 351310, Dept. Earth & Space Sciences, Seattle, WA 98195, USA

<sup>b</sup> Polar Science Center, Applied Physics Laboratory, University of Washington, Seattle, WA, USA

Received 17 December 2014; accepted in revised form 12 June 2015; Available online 30 June 2015

## Abstract

The Wet Chemistry Laboratory (WCL) on the Mars *Phoenix Lander* measured ions in a soil–water extraction and found  $\text{Na}^+$ ,  $\text{K}^+$ ,  $\text{H}^+$  (pH),  $\text{Ca}^{2+}$ ,  $\text{Mg}^{2+}$ ,  $\text{SO}_4^{2-}$ ,  $\text{ClO}_4^-$ , and  $\text{Cl}^-$ . Equilibrium models offer insights into salt phases that were originally present in the Phoenix soil, which dissolved to form the measured WCL solution; however, there are few experimental datasets for single cation perchlorates ( $\text{ClO}_4^-$ ), and none for mixed perchlorates, at low temperatures, which are needed to build models. In this study, we measure ice and salt solubilities in binary and ternary solutions in the Na-Ca-Mg- $\text{ClO}_4$  system, and then use this data, along with existing data, to construct a low-temperature Pitzer model for perchlorate brines. We then apply our model to a nominal WCL solution. Previous studies have modeled either freezing of a WCL solution or evaporation at a single temperature. For the first time, we model evaporation at subzero temperatures, which is relevant for dehydration conditions that might occur at the Phoenix site. Our model indicates that a freezing WCL solution will form ice,  $\text{KClO}_4$ , hydromagnesite ( $3\text{MgCO}_3 \cdot \text{Mg(OH)}_2 \cdot 3\text{H}_2\text{O}$ ), calcite ( $\text{CaCO}_3$ ), meridianiite ( $\text{MgSO}_4 \cdot 11\text{H}_2\text{O}$ ),  $\text{MgCl}_2 \cdot 12\text{H}_2\text{O}$ ,  $\text{NaClO}_4 \cdot 2\text{H}_2\text{O}$ , and  $\text{Mg}(\text{ClO}_4)_2 \cdot 6\text{H}_2\text{O}$  at the eutectic (209 K). The total water held in hydrated salt phases at the eutectic is ~1.2 wt.%, which is much greater than hydrated water contents when evaporation is modeled at 298.15 K (~0.3 wt.%). Evaporation of WCL solutions at lower temperatures (down to 210 K) results in lower water activities and the formation of more dehydrated minerals, e.g. kieserite ( $\text{MgSO}_4 \cdot \text{H}_2\text{O}$ ) instead of meridianiite. Potentially habitable brines, with water activity  $a_w > 0.6$ , can occur when soil temperatures are above 220 K and when the soil liquid water content is greater than 0.4 wt.% ( $100 \times g_{\text{H}_2\text{O}} g_{\text{soil}}^{-1}$ ). In general, modeling indicates that mineral assemblages derived from WCL-type solutions are characteristic of the soil temperature, water content, and water activity conditions under which they formed, and are useful indicators of past environmental conditions.

© 2015 Elsevier Ltd. All rights reserved.

## 1. INTRODUCTION

Salts found in Martian soils have broad implications for the aqueous history and habitability of Mars because salts often form via aqueous processes and their composition indicates critical habitability parameters such as pH and water activity ( $a_w$ ). Orbital spectra and *in situ*

measurements by rovers have identified a variety of salts on Mars, including chlorides (Osterloo et al., 2008; Ruesch et al., 2012), sulfates (Gendrin et al., 2005; Langevin et al., 2005; Murchie et al., 2009; Bish et al., 2013), and carbonates (Bandfield et al., 2003; Ehlmann et al., 2008; Morris et al., 2010; Niles et al., 2013). Perchlorates have also been measured in soils by the Wet Chemistry Laboratory (WCL) experiment on the *Phoenix Lander* (Hecht et al., 2009), and elsewhere by pyrolysis experiments on the *Curiosity Rover* (Leshin et al., 2013; Ming et al., 2013) and the *Viking Landers*

\* Corresponding author. Tel.: +1 267 604 3488.  
E-mail address: toner2@uw.edu (J.D. Toner).

(Navarro-González et al., 2010). Other salt species that may be present, but have not yet been detected, include chlorates and nitrates, which commonly occur in combination with perchlorate on Earth (Kounaves et al., 2010c, 2014a; Hanley et al., 2012). Salts in the upper soil surface on Mars are likely globally distributed by wind and dust storms (Yen et al., 2005). Hence, salts measured in fines in one locality likely have global implications for the soil chemistry.

The WCL experiment on the *Phoenix Lander* conducted the most comprehensive and direct analysis of the soil soluble salt content on Mars by measuring dissolved ions in a 1:25 soil–water extraction using an array of Ion Selective Electrodes (ISEs) (Hecht et al., 2009). The WCL experiment found that salts in the soil contain  $\text{Na}^+$ ,  $\text{K}^+$ ,  $\text{Ca}^{2+}$ ,  $\text{Mg}^{2+}$ ,  $\text{SO}_4^{2-}$ ,  $\text{ClO}_4^-$ , and  $\text{Cl}^-$ , and that the soil pH is alkaline (Kounaves et al., 2010a,b; Toner et al., 2014b). Ions measured in the WCL experiment dissolved from parent salts originally present in the soil and indicate broad classes of salts present, such as sulfates and perchlorates; however, the precise identity of these parent salts remains uncertain because anions and cations measured in the WCL experiment can be combined in a number of non-unique combinations. For example, perchlorate could be present as  $\text{KClO}_4$ ,  $\text{NaClO}_4 \cdot \text{nH}_2\text{O}$ ,  $\text{Mg}(\text{ClO}_4)_2 \cdot \text{nH}_2\text{O}$ , or  $\text{Ca}(\text{ClO}_4)_2 \cdot \text{nH}_2\text{O}$ , each of which has different implications for the past aqueous history and the potential for stable brines to form in soils (Marion et al., 2010; Kounaves et al., 2014b).

If we assume that salts in the soil were once dissolved in liquid water, then they would have precipitated from solution through either freezing or evaporation. Evidence for past liquid water includes a relatively high abundance of carbonate (Boynton et al., 2009) and spectrally-inferred patches of perchlorate that were likely distributed by aqueous processes (Cull et al., 2010, 2014). Starting from an initial WCL type solution, equilibrium models have been used to predict salt assemblages that form during either freezing or evaporation (Hanley et al., 2012; Marion et al., 2010; Toner et al., 2014b, 2015). Probably the most rigorous method for modeling concentrated salt equilibria is the Pitzer model, which has proven successful in a variety of settings on Earth (Harvie and Weare, 1980; Spencer et al., 1990). Pitzer models are constructed using experimental data in binary and ternary solutions (a binary solution is comprised of a single salt dissolved in water), and can then be used to model more complex brine mixtures (Pitzer, 1991).

Marion et al. (2010) developed the first comprehensive Pitzer model for perchlorates by incorporating perchlorates into FREZCHEM (Marion and Kargel, 2008). Perchlorate chemical parameters in FREZCHEM are based primarily on binary solutions, and many parameters governing more complex mixtures are assumed to be equivalent to ‘analogous salt systems’ or are set to zero. Recently, Toner et al. (2015) revised the model of Marion et al. (2010) using experimental solubility data in multicomponent perchlorate systems at 298.15 K, and found that model predictions in FREZCHEM can be greatly in error, particularly for saturated  $\text{Na}-\text{Cl}-\text{ClO}_4$ ,  $\text{Na}-\text{Mg}-\text{ClO}_4$ ,  $\text{Ca}-\text{Cl}-\text{ClO}_4$ , and

$\text{Na}-\text{SO}_4-\text{ClO}_4$  mixtures. With respect to lower temperatures, Toner et al. (2014b) used FREZCHEM to model WCL solutions during freezing and found several anomalous model predictions. For example,  $\text{Mg}^{2+}$  ion activity coefficients in  $\text{Ca}-\text{Mg}-\text{ClO}_4$  mixtures can be in excess of  $10^5$  at low-temperatures leading to anomalous ‘salting in’ and ‘salting out’ effects (‘salting in’ is an increase in solubility due to a decrease in ion activity, whereas ‘salting out’ is a decrease in solubility due to an increase in ion activity). This suggests that low-temperature perchlorate chemistries in FREZCHEM are also in need of revision.

Experimental data needed to build low-temperature Pitzer models for perchlorate brines are often either lacking or have been measured using relatively inaccurate methods. For binary perchlorate solutions, the freezing-point depression (FPD) of ice has been measured with great care and accuracy up to 1 molal concentration (this corresponds to FPDs up to  $\sim 8$  K) by Scatchard et al. (1934) ( $\text{KClO}_4$  and  $\text{NaClO}_4$ ) and Nicholson and Felsing (1950) ( $\text{Mg}(\text{ClO}_4)_2$  and  $\text{Ca}(\text{ClO}_4)_2$ ). FPDs at lower temperatures have been primarily determined using dynamic methods, in which the temperature is raised or lowered at a constant rate until ice either precipitates or melts completely (e.g. Dobrynina et al., 1980; Pestova et al., 2005). However, dynamic methods may give inaccurate FPDs at low temperatures due to slow reaction kinetics (Toner et al., 2014a). This is problematic because even small systematic errors in FPDs can result in exponential changes in modeled ion activity coefficients (Toner et al., 2014b). Furthermore, there are disagreements between different low-temperature datasets. Dobrynina et al. (1980) and Pestova et al. (2005) have measured the  $\text{Mg}(\text{ClO}_4)_2$  eutectic at 205 K, whereas Stillman and Grimm (2011) and Toner et al. (2014a) have measured the eutectic at 216 K. Similarly, Dobrynina et al. (1984) and Pestova et al. (2005) disagree on both the eutectic and salt solubilities in  $\text{Ca}(\text{ClO}_4)_2$  solutions. With respect to mixtures of perchlorate salts, no experimental data is available below 298.15 K.

The goal of this study is to address the general lack of experimental data for low-temperature perchlorates, as well as potential inaccuracies in experimental methods and disagreements between different datasets. We do this by accurately measuring FPDs of ice and salt solubilities in the  $\text{Na}-\text{Ca}-\text{Mg}-\text{ClO}_4$  system, and then use this data to extend the 298.15 K Pitzer model of Toner et al. (2015) to lower temperatures. We then apply our model to a nominal WCL solution to predict equilibrium salt assemblages in Martian soils during both freezing and evaporation. Finally, we use the model to consider the stability regions of sulfates, chlorides, and perchlorates in terms of temperature and residual soil water content.

## 2. METHODS: FPD AND SOLUBILITY MEASUREMENTS

To measure FPDs and salt solubilities, we equilibrated mixtures of either ice and solution, or salt and solution, within a copper reaction vessel at constant temperature, removing subsamples of solution periodically for later gravimetric analysis of the salt content (Fig. 1). Our equilibrium

method of measuring FPD and solubility is in contrast to dynamic methods (e.g. Pestova et al., 2005), in which the temperature is raised or lowered until the solid phase dissolves or precipitates. To prevent the salt solutions from corroding the copper, the interior of the reaction vessel ( $75\text{ cm}^3$  volume) was lined with polyethylene. The temperature of the reaction vessel was measured using a Lakeshore PT-111 Platinum Resistance Thermometer (PRT) tightly embedded within the vessel walls, and the temperature of the solution-ice mixture was measured using a Lakeshore 304 stainless steel PRT probe calibrated to an accuracy of  $\pm 0.02\text{ K}$ , which was NIST-traceable. We periodically checked the calibration of the PRT probe with a stirred ice bath. To control the temperature of the copper reaction vessel, we used a Lakeshore model 340 Cryogenic Temperature Controller. The temperature controller monitors the temperature in the vessel wall and adjusts the power output to two  $25\text{ W}$  cartridge heaters embedded within the vessel using a Proportional-Integral-Derivative (PID) control loop. To cool the vessel, we partly immersed the vessel in a liquid nitrogen bath. Using this setup, we were able to control temperatures in the reaction vessel to a precision of  $\pm 0.001\text{ K}$ . To ensure equilibrium conditions within the solution mixture, we stirred the mixture using an overhead Teflon stirrer powered by an electric motor. Subsamples of the stirred solution were periodically collected in a syringe using plastic tubing, which had  $40\text{ }\mu\text{m}$  mesh at the end so that the solid phase was excluded. The sampling tube was located within  $1\text{ cm}$  of the PRT probe to ensure that the sample temperature was accurately recorded.

During a typical experimental run, we first placed a salt solution of approximately eutectic concentration in the reaction vessel and cooled the vessel to the eutectic temperature of the salt. We then initiated crystallization of ice or salt by injecting deionized water into the solution or adding crystalline salts. After visually inspecting the solution-ice or

solution-salt mixture to ensure that a solid phase was present (ice or salt) and that the solution was being well-mixed by the stirrer, we allowed the temperature to stabilize. Once the temperature stabilized to within  $\pm 0.001\text{ K}$ , we removed  $\sim 1.5\text{ ml}$  of solution from the vessel using a syringe. The temperature of the solution mixture was then raised in increments of  $\sim 5\text{ K}$  by adjusting the temperature using the temperature controller.

Salt contents in the sampled solutions were measured gravimetrically in a vacuum oven. Approximately  $0.2\text{ ml}$  of solution was weighed out into glass vials with loose-fitting glass caps, which prevented the salt solutions from splattering out of the vials during drying and prevented absorption of water vapor during weighing. The precision of our scale is  $0.01\text{ mg}$ . The glass vials were then placed within a vacuum oven for one day at a temperature of  $\sim 500\text{ K}$  and a pressure of  $0.02\text{ mbar}$ . After allowing the vials to cool under vacuum, the vials were reweighed to determine the water loss. Repeated cycles of drying and weighing indicated that one day of drying in the vacuum oven was sufficient to fully dehydrate the solutions. Furthermore, replicate measurements of salt concentration using the above methods gave results consistent within  $\pm 0.01\text{ mol kg}^{-1}$ .

Chemicals used in this study were  $\text{Mg}(\text{ClO}_4)_2 \cdot 6\text{H}_2\text{O}$  (99%),  $\text{Ca}(\text{ClO}_4)_2 \cdot 4\text{H}_2\text{O}$  (99%), and ACS reagent grade  $\text{NaClO}_4 \cdot \text{H}_2\text{O}$  (98%) from Sigma-Aldrich®. For solubilities in the binary  $\text{Mg}(\text{ClO}_4)_2$ ,  $\text{Ca}(\text{ClO}_4)_2$ , and  $\text{NaClO}_4$  systems, these salts were further purified by filtering at  $0.45\text{ }\mu\text{m}$  and recrystallization. No further purification was done for the ternary salt systems. The perchlorate mixtures were made from binary stock solutions of known concentration, mixed so that each binary component in the mixture contributed a roughly equal molar amount of perchlorate. Given that the formation of ice will not change the ratio of component salts in a ternary mixture, we were

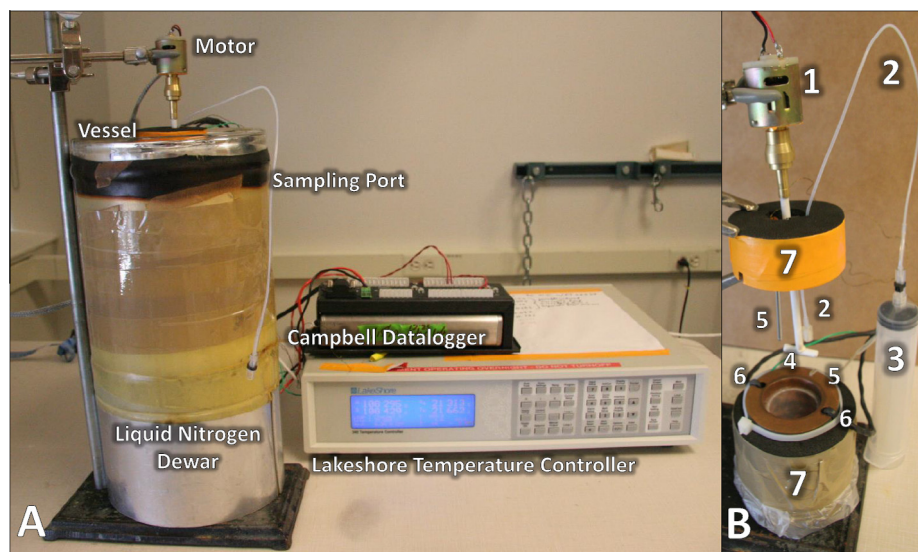


Fig. 1. The experimental setup used to measure solubilities. (A) The configuration of the experiment during sample runs. (B) Different components of the experimental setup, showing: (1) the electric motor, (2) sampling tubing, (3) sample syringe, (4) Teflon stirrer, (5) stainless steel encased PRT, (6) cartridge heaters, and (7) vessel body/cap.

able to measure salt concentrations in ternary samples gravimetrically by assuming a constant ratio for the component salts.

To calculate water activities from our FPD measurements, we use the FREZCHEM equation relating water activity to temperature up to 272.15 K (Marion and Kargel, 2008):

$$a_w = 1.906354 - (1.880285 \times 10^{-2})T + (6.603001 \times 10^{-5})T^2 - (3.419967 \times 10^{-8})T^3 \quad (1)$$

Eq. (11) performs poorly near 273.15 K, leading to erroneous values for the osmotic coefficient, so above 272.15 K we calculate  $a_w$  as (Robinson and Stokes, 1959):

$$\log a_w = 0.004207(273.15 - T) + 2.1 \times 10^{-6}(273.15 - T)^2 \quad (2)$$

### 3. ICE AND SALT SOLUBILITY RESULTS

FPDs measured in other studies are generally consistent with our measurements within a few degrees (Table 1, Fig. 2). In NaClO<sub>4</sub> solutions, FPDs measured by Hennings et al. (2013) and Freeth (1924) sometimes differ from our measurements by up to six degrees at the same molality. In Ca(ClO<sub>4</sub>)<sub>2</sub> solutions, the data of Pestova et al. (2005) is scattered above and below our dataset by an average of about one degree. The data of Dobrynina et al. (1984) is also consistent with our dataset at low molality, but differs significantly from both our study and Pestova et al. (2005) above  $\sim$ 6 mol kg<sup>-1</sup>. In Mg(ClO<sub>4</sub>)<sub>2</sub> solutions, FPDs determined in our study, Pestova et al. (2005), and Dobrynina et al. (1980) are all consistent to within a few degrees. The new results of FPDs in ternary perchlorate mixtures are approximately midway between

FPDs determined in the component binary salts (Fig. 2D). Stillman and Grimm (2011) and Toner et al. (2014a,b) suggested that the ‘visual polythermal method’ of measuring FPDs, during which salt solutions are slowly cooled until visual inspection identifies ice precipitation (Dobrynina et al., 1980; Dobrynina et al., 1984; Pestova et al., 2005), may systematically underestimate FPDs due to supercooling. However, FPDs measured with the ‘visual polythermal method’ do not lie systematically below our equilibrium measurements, as would be expected from supercooling.

Our solubility results are also generally similar to previous measurements (Table 2, Fig. 2A–C). NaClO<sub>4</sub> solubilities in our study agree well with the compilation of Chan et al. (1995), which is based on multiple solubility measurements at each temperature, and Chretien and Kohlmuller (1966). Data from the study of Hennings et al. (2013), which measured FPDs using a dynamic method, are scattered relative to our measurements by up to  $\pm 10$  K. Mg(ClO<sub>4</sub>)<sub>2</sub> solubilities in our study are consistent with both Dobrynina et al. (1980) and Pestova et al. (2005), although we find that Mg(ClO<sub>4</sub>)<sub>2</sub> is less soluble near the eutectic. We assume that Mg(ClO<sub>4</sub>)<sub>2</sub>·6H<sub>2</sub>O forms at all temperatures because Mg(ClO<sub>4</sub>)<sub>2</sub>·6H<sub>2</sub>O is the stable phase at 298.15 K and there are no obvious phase transitions in our solubility data. Pestova et al. (2005) indicates that the hydration state is 8H<sub>2</sub>O at all temperatures, but this is inconsistent with the 6H<sub>2</sub>O hydration state at 298.15 K determined by many separate investigators (Chan et al., 1989).

$\text{Ca}(\text{ClO}_4)_2$  solubilities in our study are consistent with Pestova et al. (2005), but are much lower than solubilities in Dobrynina et al. (1984) above 250 K. Possibly, Dobrynina et al. (1984) measured metastable phases above 250 K. There has been some disagreement on the low temperature hydration state of  $\text{Ca}(\text{ClO}_4)_2$  salts (6H<sub>2</sub>O or

Table 1

Table 1  
Experimental FPD measurements determined in this study, with temperature in Kelvin and molal ( $\text{mol kg}^{-1}$ ) ion concentrations. A single measurement was done at each temperature.

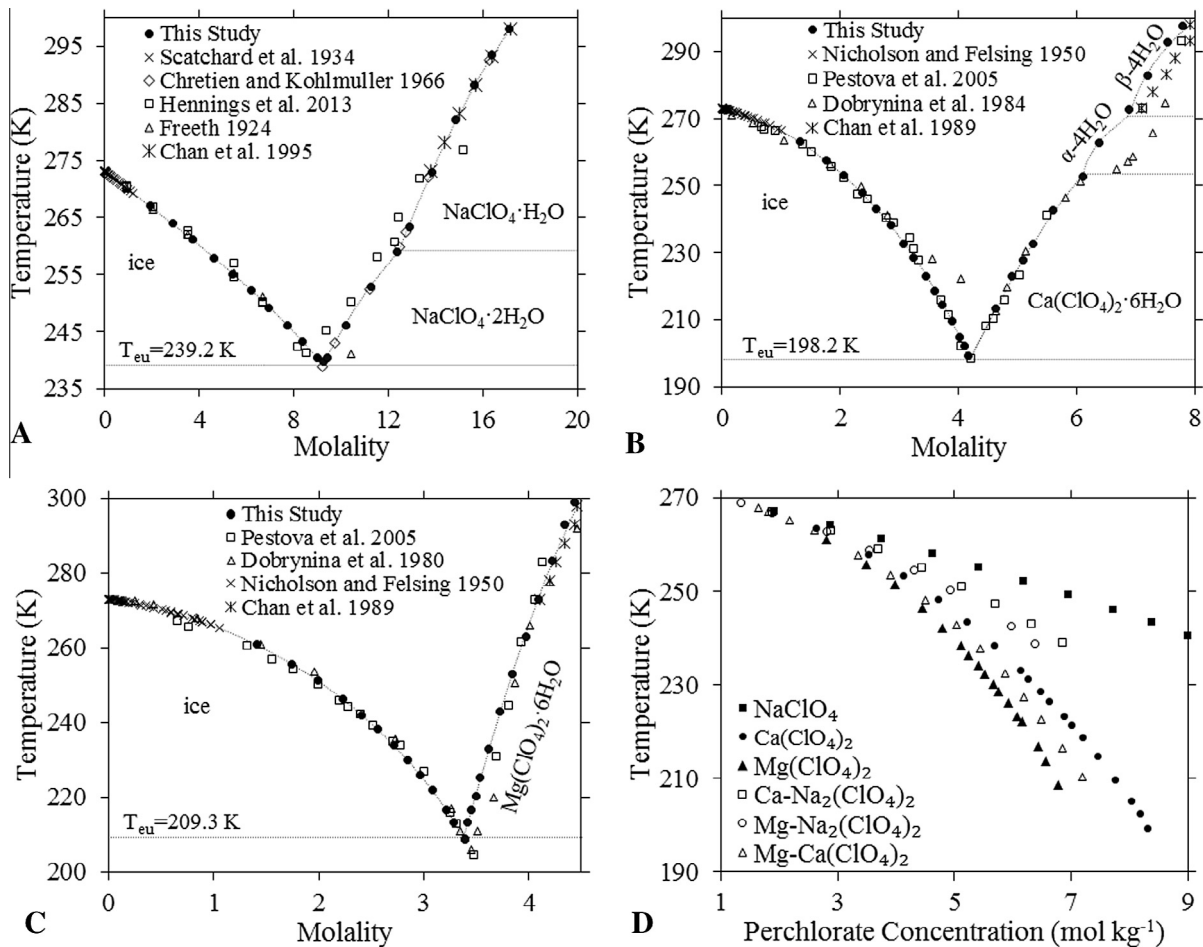


Fig. 2. Ice and salt solubilities determined in this study and from previous studies for NaClO<sub>4</sub> (A), Ca(ClO<sub>4</sub>)<sub>2</sub> (B), Mg(ClO<sub>4</sub>)<sub>2</sub> (C), and ternary mixtures (open symbols) compared to binary solutions (closed symbols) (D). The dotted lines indicate ice solubilities, salt solubilities, and eutectic temperatures modeled in this study.

Table 2

Experimental solubility measurements determined in this study, with temperature in Kelvin and molal (mol kg<sup>-1</sup>) ion concentrations. A single measurement was done at each temperature.

Temp.	NaClO <sub>4</sub>	Temp.	Ca(ClO <sub>4</sub> ) <sub>2</sub>	Temp.	Mg(ClO <sub>4</sub> ) <sub>2</sub>
239.67	9.274	213.41	4.629	209.15	3.395
240.47	9.397	222.91	4.914	213.20	3.420
246.11	10.193	227.88	5.104	216.71	3.451
252.84	11.259	232.87	5.260	220.43	3.495
258.90	12.347	242.89	5.609	225.47	3.540
263.45	12.916	252.87	6.098	232.95	3.617
273.02	13.865	262.97	6.371	242.95	3.720
282.07	14.861	272.97	6.895	252.94	3.840
288.18	15.648	282.98	7.199	262.92	3.973
293.47	16.383	292.94	7.548	273.00	4.093
298.01	17.083	297.93	7.800	283.45	4.221
				292.85	4.339
				298.90	4.441

4H<sub>2</sub>O (Dobrynina et al., 1984; Pestova et al., 2005), but a recent analysis by Hennings et al. (2014) indicates that Ca(ClO<sub>4</sub>)<sub>2</sub>·6H<sub>2</sub>O is the stable phase at 238 K and that

Ca(ClO<sub>4</sub>)<sub>2</sub>·4H<sub>2</sub>O is the stable phase between 273.15 and >298.15 K. Our solubility data suggests that there are several kinks in the solubility curve between 250 and 273 K,

which correlate well with phase transitions inferred by Toner et al. (2014a) at 253.6 K and 270.8 K. We assume here that the phase transition at 253.6 K is due to the dehydration of  $\text{Ca}(\text{ClO}_4)_2 \cdot 6\text{H}_2\text{O}$  to  $\alpha\text{-Ca}(\text{ClO}_4)_2 \cdot 4\text{H}_2\text{O}$ . Then, by analogy to the aqueous  $\text{CaCl}_2$  system, which has multiple polymorphs of  $\text{CaCl}_2 \cdot 4\text{H}_2\text{O}$  (Pátek et al., 2008), we assume that the phase transition at 270.8 K is due to the formation of  $\beta\text{-Ca}(\text{ClO}_4)_2 \cdot 4\text{H}_2\text{O}$ . We note that the hydration state of  $\text{Ca}(\text{ClO}_4)_2$  has no effect on our Pitzer model parameterization, which is based on FPD measurements, but does influence the calculated solubility product. If the hydration state of  $\text{Ca}(\text{ClO}_4)_2$  is found to differ in subsequent studies, it is a simple matter to add an additional salt phase to the Pitzer model by calculating its solubility product.

#### 4. THERMODYNAMIC MODELING

##### 4.1. Pitzer model

Fundamentally, the Pitzer equations are described by binary Pitzer parameters  $\beta^{(0)}$ ,  $\beta^{(1)}$ ,  $\beta^{(2)}$ , and  $C^\phi$  (describing single-salt aqueous solutions), and the ternary parameters  $\theta$  and  $\psi$  (describing mixtures of two salts), which are functions of temperature and pressure. The temperature dependence of these parameters for perchlorates is determined from experimental data, as explained below. In this study, we use the Pitzer approach of FREZCHEM v.13.3 (Marion and Kargel, 2008), which gives the osmotic coefficient ( $\phi$ ) and ion activity coefficients ( $\gamma$ ) for cations ( $M$ ) and anions ( $X$ ) in a mixed salt solution (excluding neutral species for simplicity) as:

$$\begin{aligned}\phi = 1 + \frac{2}{\sum m_i} & \left\{ \frac{-A_\phi I^{3/2}}{1 + b\sqrt{I}} + \sum \sum m_c m_a (\beta_{ca}^\phi + ZC_{ca}) \right. \\ & + \sum \sum m_c m_{c'} (\Phi_{cc'}^\phi + \sum m_a \psi_{cc'a}) \\ & \left. + \sum \sum m_a m_{a'} (\Phi_{aa'}^\phi + \sum m_c \psi_{aad'c}) \right\} \quad (3)\end{aligned}$$

$$\begin{aligned}\ln \gamma_M = z_M^2 F + \sum m_a (2\beta_{Ma} + ZC_{Ma}) + \sum m_c (2\Phi_{Mc} \\ + \sum m_a \psi_{Mca}) + \sum \sum m_a m_{a'} \psi_{Maa'} \\ + |z_M| \sum \sum m_c m_a C_{ca} \quad (4)\end{aligned}$$

$$\begin{aligned}\ln \gamma_X = z_X^2 F + \sum m_c (2\beta_{cX} + ZC_{cX}) + \sum m_a (2\Phi_{Xa} \\ + \sum m_c \psi_{Xac}) + \sum \sum m_c m_{c'} \psi_{cc'X} \\ + |z_X| \sum \sum m_c m_a C_{ca} \quad (5)\end{aligned}$$

where  $m$  (mol kg<sup>-1</sup>) is the molality of cations ( $c$  and  $c'$ ) and anions ( $a$  and  $a'$ ),  $z$  is the ion charge,  $I$  is the ionic strength,  $A_\phi$  is the Debye–Hückel limiting law slope (0.3917 kg<sup>1/2</sup> · mol<sup>-1/2</sup> at 298.15 K),  $b$  is a constant (1.2 kg<sup>-1/2</sup> mol<sup>-1/2</sup>), and  $Z = \sum m_i |z_i|$ . The functions  $\beta^\phi$ ,  $\beta$ ,  $C$ ,  $\Phi^\phi$ , and  $\Phi$  are given by:

$$\beta_{MX}^\phi = \beta_{MX}^{(0)} + \beta_{MX}^{(1)} \exp(-\alpha_1 \sqrt{I}) + \beta_{MX}^{(2)} \exp(-\alpha_2 \sqrt{I}) \quad (6)$$

$$\beta_{MX} = \beta_{MX}^{(0)} + \beta_{MX}^{(1)} g(-\alpha_1 \sqrt{I}) + \beta_{MX}^{(2)} g(-\alpha_2 \sqrt{I}) \quad (7)$$

$$C_{MX} = \frac{C_{MX}^\phi}{2\sqrt{|z_M z_X|}} \quad (8)$$

$$\Phi_{ij}^\phi = \theta_{ij} + {}^E\theta_{ij} + I \frac{d^E \theta_{ij}}{dl} \quad (9)$$

$$\Phi_{ij} = \theta_{ij} + {}^E\theta_{ij} \quad (10)$$

where  $i$  and  $j$  indicate different cation–cation or anion–anion pairs. For 1–1 (e.g. NaCl) or 1–2 salts (e.g.  $\text{CaCl}_2$ ),  $\alpha_1 = 2$  and  $\alpha_2 = 0 \text{ kg}^{-1/2} \text{ mol}^{-1/2}$ ; for 2–2 salts (e.g.  $\text{MgSO}_4$ ),  $\alpha_1 = 1.4$  and  $\alpha_2 = 12 \text{ kg}^{-1/2} \text{ mol}^{-1/2}$ .  ${}^E\theta_{ij}$  is a ionic strength dependent higher-order electrostatic term accounting for interactions between pairs of anions or cations having different charges (if  $z_i = z_j$ ,  ${}^E\theta_{ij}$  equals zero).  $g(x)$  is a function given by:

$$g(x) = \frac{2}{x^2} [1 - (1+x) \exp(-x)] \quad (11)$$

$F$  is a function given by:

$$\begin{aligned}F = -A_\phi & \left[ \frac{\sqrt{I}}{1+b\sqrt{I}} + \frac{2}{b} \ln(1+b\sqrt{I}) \right] \\ & + \sum \sum m_c m_a \beta'_{ca} + \sum \sum m_c m_{c'} \Phi'_{cc'} \\ & + \sum \sum m_a m_{a'} \Phi'_{aa'} \quad (12)\end{aligned}$$

where the prime symbols on  $\beta$  and  $\Phi$  indicate differentiation with respect to ionic strength. Finally, the osmotic coefficient in Eq. (3) is related to the water activity of a solution ( $a_w$ ) by:

$$a_w = \exp\left(\frac{-\phi \sum m_i}{55.50844}\right) \quad (13)$$

For a more detailed explanation of the FREZCHEM Pitzer implementation, particularly if neutral species are included, see Marion and Kargel (2008).

The change in Pitzer parameters  $\beta^{(0)}$ ,  $\beta^{(1)}$ , and  $C^\phi$  with temperature at temperature  $T$  (Kelvin) can be determined from the apparent relative molar enthalpy ( ${}^\phi L$ ) in binary solutions by the equation (Silvester and Pitzer, 1978):

$${}^\phi L = v|z_c z_a| A_H \frac{\ln(1+b\sqrt{I})}{2b} - 2v_c v_a RT^2 [m \beta_{ca}^L + v_c v_a m^2 C_{ca}^L] \quad (14)$$

where  $A_H$  is the Debye–Hückel slope for enthalpy ( $A_H/RT = 0.7956 \text{ kg}^{1/2} \text{ mol}^{-1/2}$  at 298.15 K),  $v_c$  and  $v_a$  are stoichiometric numbers of cations or anions ( $v = v_c + v_a$ ),  $R$  is the universal molar gas constant,  $\beta^L$  is a function of  $\beta^{L(0)}$ ,  $\beta^{L(1)}$ , and  $\beta^{L(2)}$  (analogous to Eq. (7)), and  $C^L$  is a function of  $C^{L\phi}$  (analogous to Eq. (8)). The empirical fitting parameters  $\beta^{L(0)}$ ,  $\beta^{L(1)}$ ,  $\beta^{L(2)}$ , and  $C^{L\phi}$  are related to Pitzer–ion interaction parameters  $\beta^{(0)}$ ,  $\beta^{(1)}$ ,  $\beta^{(2)}$ , and  $C^\phi$  at constant temperature and pressure by:

$$\beta^{L(i)} = \frac{\partial \beta^{(i)}}{\partial T} \text{ and } C^{L\phi} = \frac{\partial C^\phi}{\partial T} \quad (15)$$

To describe the temperature dependence of Pitzer parameters ( $P$ ) and log solubility products ( $\ln K$ ) governing Na–Mg–Ca–ClO<sub>4</sub> solutions, we use the equation:

$$P = \ln K = A + B(T - 298.15) + C(T - 298.15)^2 \quad (16)$$

where  $A$  is the parameter value at 298.15 K,  $B$  is the change with temperature at 298.15 K, and  $C$  is an empirical fitting parameter. Parameter  $P$  can be either  $\beta^{(0)}$ ,  $\beta^{(1)}$ ,  $C^\phi$ ,  $\theta$ , or  $\psi$ . The Na-Mg-Ca-ClO<sub>4</sub> system is described by the binary Pitzer parameters  $\beta^{(0)}$ ,  $\beta^{(1)}$ , and  $C^\phi$  for NaClO<sub>4</sub>, Mg(ClO<sub>4</sub>)<sub>2</sub>, and Ca(ClO<sub>4</sub>)<sub>2</sub> solutions (six parameters total), the cation–cation parameters  $\theta_{\text{Mg}^{2+}, \text{Na}^+}$ ,  $\theta_{\text{Ca}^{2+}, \text{Na}^+}$ , and  $\theta_{\text{Mg}^{2+}, \text{Ca}^{2+}}$ , and the ternary parameters  $\psi_{\text{Mg}^{2+}, \text{Na}^+, \text{ClO}_4^-}$ ,  $\psi_{\text{Ca}^{2+}, \text{Na}^+, \text{ClO}_4^-}$ , and  $\psi_{\text{Mg}^{2+}, \text{Na}^{2+}, \text{ClO}_4^-}$ . Eq. (16) is used to fit only  $\beta^{(0)}$ ,  $\beta^{(1)}$ ,  $C^\phi$ , and  $\psi$  parameters in the Na-Mg-Ca-ClO<sub>4</sub> system.

We assume that the all cation–cation  $\theta$  parameters have the same temperature dependence in FREZCHEM because these parameters are used in many other mixtures in FREZCHEM; hence, reevaluating these parameters would require the simultaneous reevaluation of nearly all chemistries in the FREZCHEM model, which is beyond the scope of the present work. Furthermore, we note that there is little improvement to our model fits if  $\theta$  parameters are allowed to vary from their values in FREZCHEM. All other parameters and solubility products not included in the Na-Mg-Ca-ClO<sub>4</sub> system are assumed to be the same as in FREZCHEM v.13.3, including revisions at 298.15 K made by Toner et al. (2015) (with the exception of  $\theta_{\text{Cl}^-, \text{ClO}_4^-}$  and  $\psi_{\text{Na}^+, \text{Cl}^-, \text{ClO}_4^-}$  parameters, as described in Section 4.3).

We determine the coefficients  $A$ ,  $B$ , and  $C$  in Eq. (16) in the following steps:

1. We take parameter values and solubility products at 298.15 K (coefficient  $A$  in Eq. (16)) from the revised perchlorate model in Toner et al. (2015).
2. We determine the change in binary Pitzer parameters  $\beta^{(0)}$ ,  $\beta^{(1)}$ , and  $C^\phi$  with temperature at 298.15 K (coefficient  $B$  in Eq. (16)) by fitting Eq. (14) to enthalpy of solution data at 298.15 K from Vanderzee and Swanson (1963) (NaClO<sub>4</sub>, 0–17 molal), Jongenburger and Wood (1965) (Mg(ClO<sub>4</sub>)<sub>2</sub>, 0–3.2 molal), and Gier and Vanderzee (1974) (Ca(ClO<sub>4</sub>)<sub>2</sub>, 0–7.7 molal). Enthalpy of solution data is not available for perchlorate mixtures, so for ternary  $\psi$  parameters, coefficient  $B$  in Eq. (16) is treated as an additional empirical coefficient in the following step.
3. We determine the value of coefficient  $C$  in Eq. (16) for binary Pitzer parameters, and both  $B$  and  $C$  for  $\psi$  parameters, by fitting Eq. (3) to experimental FPD data. We use only the high accuracy data of Scatchard et al. (1934), Nicholson and Felsing (1950), and FPD data in this study.
4. Using the temperature-dependent Pitzer parameters determined in the steps above, we determine temperature-dependent solubility products ( $\ln K$ ) for NaClO<sub>4</sub>, Mg(ClO<sub>4</sub>)<sub>2</sub>, and Ca(ClO<sub>4</sub>)<sub>2</sub> salts. First, we calculate ion activity products (IAP) at each of the experimental salt solubility points determined in this study using Eqs. (1)–(3). Then, we fit these IAPs to Eq. (16) by varying coefficients  $B$  and  $C$ .

## 4.2. Developing a model for perchlorate brines

The temperature coefficients of the Pitzer parameters determined from  $^\phi L$  (given as  $B$  coefficient for binary parameters Table 3) indicate that  $\beta^{(0)}$ ,  $\beta^{(1)}$ , and  $C^\phi$  generally undergo small changes with temperature (Fig. 3). This is consistent with the small temperature coefficients for Pitzer parameters found in other electrolyte systems (Silvester and Pitzer, 1978). For Ca(ClO<sub>4</sub>)<sub>2</sub> and Mg(ClO<sub>4</sub>)<sub>2</sub>,  $\beta^{(0)}$  and  $\beta^{(1)}$  change by <1 % K<sup>-1</sup>, whereas these parameters change by ~1.5 % K<sup>-1</sup> for NaClO<sub>4</sub>. The  $C^\phi$  parameter undergoes the most rapid change with temperature, between 3 and 5 % K<sup>-1</sup>. The generally slow change in parameters with temperature suggests that a reasonable approximation for chemistries lacking low-temperature data is to assume constant Pitzer parameters with temperature.

For Ca(ClO<sub>4</sub>)<sub>2</sub> and Mg(ClO<sub>4</sub>)<sub>2</sub> solutions, osmotic coefficients calculated from other authors' FPDs are characterized by scattered osmotic coefficients below about 2 m, but are consistent with our study at higher concentrations, with the exception of the Ca(ClO<sub>4</sub>)<sub>2</sub> data from Dobrynina et al. (1984) (Fig. 4A and C). In contrast, osmotic coefficients in NaClO<sub>4</sub> solutions are scattered over the entire range of molality to the eutectic (Fig. 4E). The generally larger scatter found at lower molality is due to the greater sensitivity of the osmotic coefficient to errors in concentration and temperature at low concentrations. Because FREZCHEM is parameterized to this scattered data, FREZCHEM systematically overestimates osmotic coefficients at low molality.

Despite the seemingly small differences in osmotic coefficients between our model and FREZCHEM, mean ion activity coefficients predicted by FREZCHEM are much greater than in our model, particularly at low temperatures (Fig. 4B, D, and F). Our model predicts that ion activity coefficients in Ca(ClO<sub>4</sub>)<sub>2</sub> and Mg(ClO<sub>4</sub>)<sub>2</sub> solutions remain near their values at 298.15 K at all temperatures modeled (Fig. 4B and D), whereas ion activity coefficients in NaClO<sub>4</sub> decrease with temperature (Fig. 4F). Toner et al. (2014b) found that the large increase in Mg(ClO<sub>4</sub>)<sub>2</sub> ion activity coefficients in FREZCHEM causes a number of anomalous ‘salting out’ effects for salts of Mg<sup>2+</sup>. The cause of the larger ion activity coefficients predicted by FREZCHEM can be seen from the relationship between mean ion activity coefficients ( $\gamma_\pm$ ) and osmotic coefficients at constant temperature and pressure (Robinson and Stokes, 1959):

$$\ln \gamma_\pm = (\phi - 1) + \int_0^m \frac{\phi - 1}{m} dm \quad (17)$$

Eq. (17) indicates that ion activity coefficients at a given molality are an exponential function of osmotic coefficients at lower concentrations; hence, errors in the osmotic coefficient at low molality have a cumulative effect on calculated ion activity coefficients at higher molality. Generally, higher osmotic coefficients lead to exponentially higher ion activity coefficients. This indicates the importance of accurately

Table 3

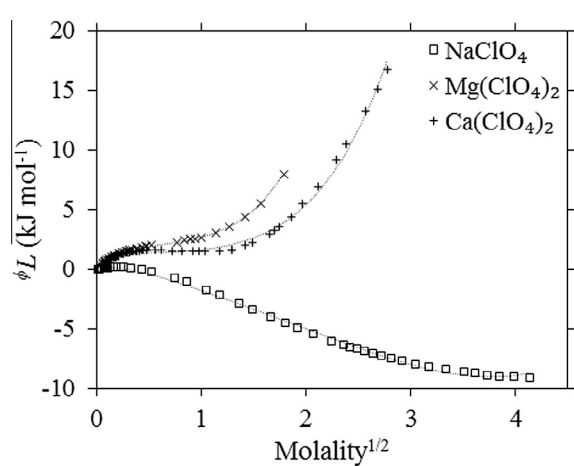
Pitzer parameters determined in this study as a function of temperature. Constants  $A$ ,  $B$ , and  $C$  are used in Eq. (7).

Parameter	$A$	$B$	$C$
$\beta_{\text{Na}^+, \text{ClO}_4^-}^{(0)}$	5.5400E–02	7.8712E–04	–3.8727E–06
$\beta_{\text{Na}^+, \text{ClO}_4^-}^{(1)}$	2.7550E–01	4.4318E–03	–1.2331E–04
$C_{\text{Na}^+, \text{ClO}_4^-}^\phi$	–1.1800E–03	–5.3394E–05	3.9507E–07
$\beta_{\text{Ca}^{2+}, \text{ClO}_4^-}^{(0)}$	4.5113E–01	3.9760E–04	5.0103E–07
$\beta_{\text{Ca}^{2+}, \text{ClO}_4^-}^{(1)}$	1.7565E + 00	7.3598E–03	–1.2439E–04
$C_{\text{Ca}^{2+}, \text{ClO}_4^-}^\phi$	–5.0010E–03	–1.6682E–04	–5.9959E–07
$\beta_{\text{Mg}^{2+}, \text{ClO}_4^-}^{(0)}$	4.9613E–01	4.9397E–04	–2.7085E–06
$\beta_{\text{Mg}^{2+}, \text{ClO}_4^-}^{(2)}$	2.0085E + 00	5.0772E–03	–4.2302E–04
$C_{\text{Mg}^{2+}, \text{ClO}_4^-}^\phi$	9.5810E–03	–3.4602E–04	–2.1062E–07
$\theta_{\text{Cl}^-, \text{ClO}_4^-}$	3.0990E–02	–1.9343E–03	–
$\psi_{\text{Mg}^{2+}, \text{Na}^+, \text{ClO}_4^-}$	–2.8310E–02	1.0937E–03	1.5821E–05
$\psi_{\text{Ca}^{2+}, \text{Na}^+, \text{ClO}_4^-}$	–1.1780E–02	9.4502E–04	1.5312E–05
$\psi_{\text{Ca}^{2+}, \text{Na}^{2+}, \text{ClO}_4^-}$	–2.2870E–02	–1.1050E–03	1.9090E–06
$\psi_{\text{Na}^+, \text{Cl}^-, \text{ClO}_4^-}$	–5.4690E–03	3.2352E–04	–

Table 4

Solubility products ( $\ln K$ ) of salt dissolution as a function of temperature. Constants  $A$ ,  $B$ , and  $C$  are used in Eq. (7).

Salt	$A$	$B$	$C$
$\text{Ca}(\text{ClO}_4)_2 \cdot 6\text{H}_2\text{O}$	1.5111E + 01	4.2120E–02	–2.1785E–04
$\alpha\text{-Ca}(\text{ClO}_4)_2 \cdot 4\text{H}_2\text{O}$	2.2682E + 01	2.9930E–01	3.0986E–03
$\beta\text{-Ca}(\text{ClO}_4)_2 \cdot 4\text{H}_2\text{O}$	1.7581E + 01	4.7534E–02	7.0030E–04
$\text{Mg}(\text{ClO}_4)_2 \cdot 6\text{H}_2\text{O}$	1.2878E + 01	8.6545E–03	–4.6569E–04
$\text{NaClO}_4 \cdot \text{H}_2\text{O}$	5.0222E + 00	2.9826E–02	–2.4587E–04
$\text{NaClO}_4 \cdot 2\text{H}_2\text{O}$	5.4008E + 00	6.3081E–02	–

Fig. 3. Experimentally derived values for  $\phi_L$  from Vanderzee and Swanson (1963) ( $\text{NaClO}_4$ ,  $\square$ ), Gier and Vanderzee (1974) ( $\text{Ca}(\text{ClO}_4)_2$ , +), and Jongenburger and Wood (1965) ( $\text{Mg}(\text{ClO}_4)_2$ , x). Modeled values using Eq. (5) are given as dotted lines.

fitting osmotic coefficient data at low molality (as seen in comparison to FREZCHEM in Fig. 4). Fortunately, the experimental studies that measured FPDs at low molality

(Scatchard et al., 1934; Nicholson and Felsing, 1950) were rigorous and put much effort into achieving high accuracy temperature and concentration measurements (see the lengthy description of experimental methods in Scatchard et al. (1932)), so we are confident in the accuracy of FPDs measured below 1 molal concentration.

Our model provides a good fit to osmotic coefficients calculated from experimental FPDs in perchlorate mixtures; in contrast, FREZCHEM predicts significantly different osmotic coefficients in  $\text{Mg-Ca}(\text{ClO}_4)_2$  and  $\text{Mg-Na}_2(\text{ClO}_4)_2$  mixtures (Fig. 5A). The differences between our model and FREZCHEM become even more apparent by comparing model predictions for ion activity coefficients (Fig. 5B). In  $\text{Mg-Ca}(\text{ClO}_4)_2$  and  $\text{Mg-Na}_2(\text{ClO}_4)_2$  mixtures, FREZCHEM predicts  $\gamma_{\text{Mg}}/\gamma_{\text{Ca}}$  and  $\gamma_{\text{Mg}}/\gamma_{\text{Na}}$  ratios that are up to several orders of magnitude greater than in our model. This is primarily caused by the extremely high ion activity coefficients in  $\text{Mg}(\text{ClO}_4)_2$  solutions predicted by FREZCHEM (Fig. 4B). Ion activity coefficient ratios are important because they control mineral stability through ‘salting in’ and ‘salting out’ effects for salts having a common ion. For example, Toner et al. (2014b) found that FREZCHEM predicts that  $\text{MgSO}_4$  salts will precipitate instead of  $\text{CaSO}_4$  salts in low-temperature  $\text{Mg}(\text{ClO}_4)_2$

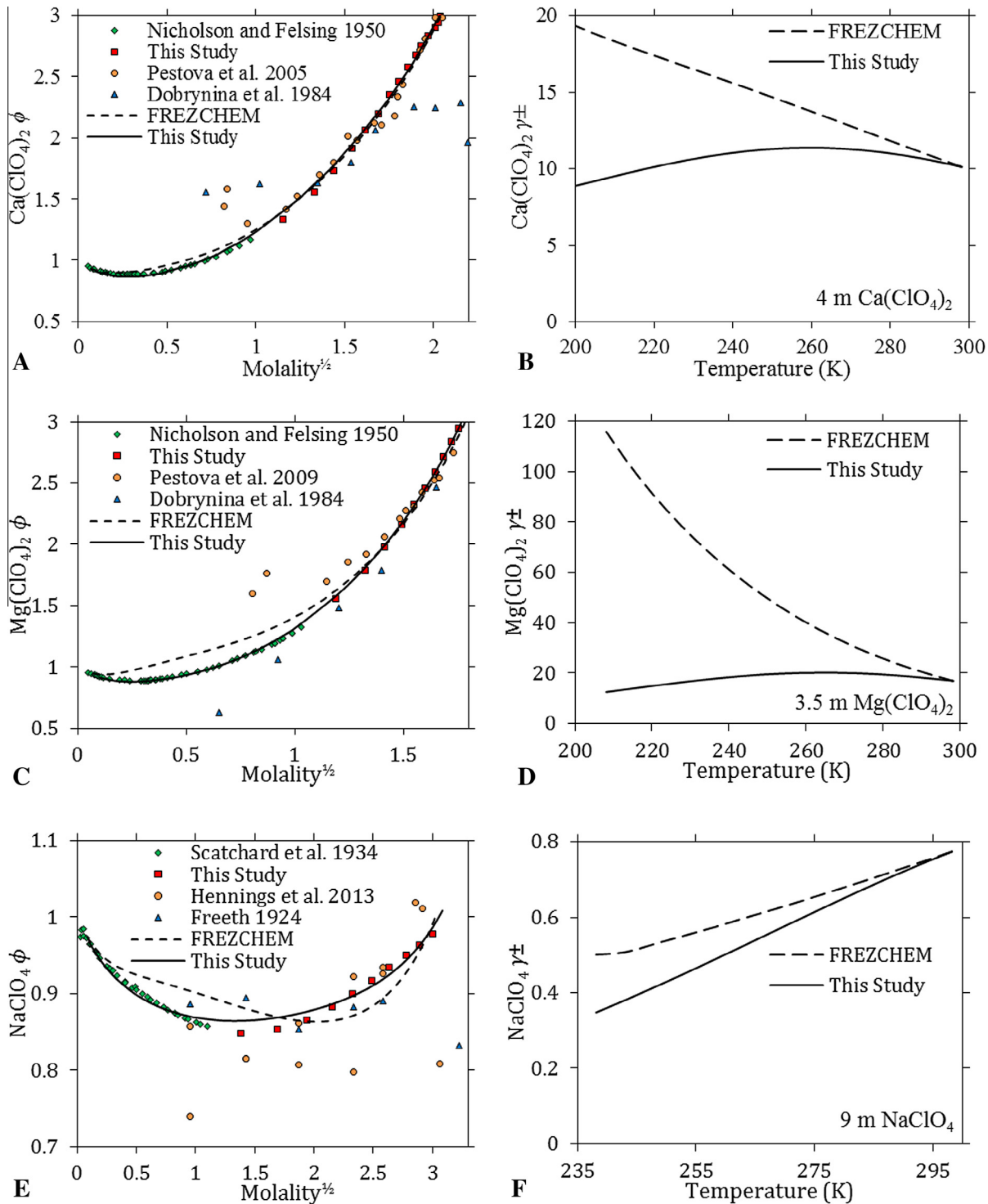


Fig. 4. Model fits (this study and FREZCHEM) to osmotic coefficients ( $\phi$ ) calculated from FPDs using Eqs. (1) or (2) for  $\text{Ca}(\text{ClO}_4)_2$ ,  $\text{Mg}(\text{ClO}_4)_2$ , and  $\text{NaClO}_4$  solutions (A, C, and E). Mean ion activity coefficients ( $\gamma_{\pm}$ ) calculated from this study and from FREZCHEM for 4 m  $\text{Ca}(\text{ClO}_4)_2$ , 3.5 m  $\text{Mg}(\text{ClO}_4)_2$ , and 9 m  $\text{NaClO}_4$  solutions (B, D, and F).

brines due to  $\gamma_{\text{Mg}}/\gamma_{\text{Ca}}$  ratios on the order of  $\sim 5000$ , leading to the formation of Ca-Mg-ClO<sub>4</sub>-rich brines. In our model,  $\gamma_{\text{Mg}}/\gamma_{\text{Ca}}$  ratios remain roughly constant, so such unusual ‘salting in/out’ effects do not occur. On the other hand, our model does predict a ‘salting out’ effect for Na

salts relative to salts of Mg and Ca due to increasing  $\gamma_{\text{Mg}}/\gamma_{\text{Na}}$  and  $\gamma_{\text{Ca}}/\gamma_{\text{Na}}$  ratios with increasing concentration.

Our model predictions for salt solubility are in good agreement with experimental data (Fig. 2A-C; Table 4; Table 5). In NaClO<sub>4</sub> solutions, Hennings et al. (2013) found

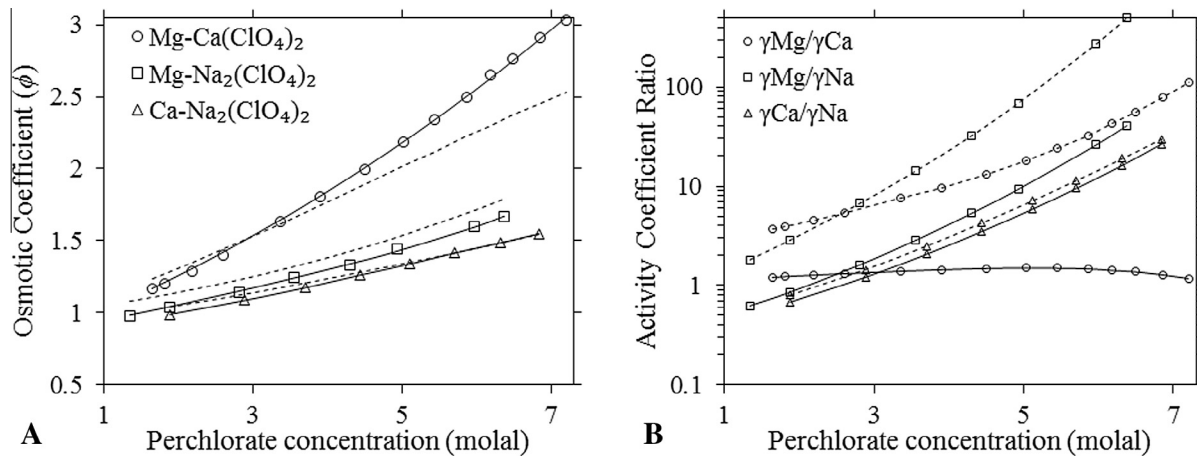


Fig. 5. Comparisons between experimental and modeled values (this study and FREZCHEM) for solutions in equilibrium with ice at various temperatures/concentrations (A and B). (A) measured osmotic coefficients for Mg-Ca(ClO<sub>4</sub>)<sub>2</sub> (○), Mg-Na<sub>2</sub>(ClO<sub>4</sub>)<sub>2</sub> (□), and Ca-Na<sub>2</sub>(ClO<sub>4</sub>)<sub>2</sub> (Δ) mixtures from FPD measurements compared to modeled values from this study (—) and FREZCHEM (----). (B) A comparison between modeled ion activity coefficient ratios in this study (—) and FREZCHEM (----) for Mg-Ca(ClO<sub>4</sub>)<sub>2</sub> (○  $\gamma_{\text{Mg}}/\gamma_{\text{Ca}}$ ), Mg-Na<sub>2</sub>(ClO<sub>4</sub>)<sub>2</sub> (□  $\gamma_{\text{Mg}}/\gamma_{\text{Na}}$ ), and Ca-Na<sub>2</sub>(ClO<sub>4</sub>)<sub>2</sub> (Δ  $\gamma_{\text{Ca}}/\gamma_{\text{Na}}$ ) mixtures in Fig. 5A. Note: for all salt mixtures, the individual salt components contribute an equal amount of ClO<sub>4</sub>.

that there is a stable eutectic at 239.05 K and a metastable eutectic at 237.35 K; our model is consistent with the stable eutectic. In Ca(ClO<sub>4</sub>)<sub>2</sub> solutions, our modeled eutectic (198.2 K) is similar to the experimental eutectic found by Pestova et al. (2005) (198.55 K); in contrast, Dobrynina et al. (1984) found that the Ca(ClO<sub>4</sub>)<sub>2</sub> eutectic is 212.65 K. FPDs measured near the eutectic by Dobrynina et al. (1984) are also much higher than in this study or Pestova et al. (2005), and we find that if this data is used to fit a Pitzer model, the resulting model predicts implausibly high ion activity coefficients ( $>10^5$ ). This suggests that there may be experimental or typographic errors in the study of Dobrynina et al. (1984). In Mg(ClO<sub>4</sub>)<sub>2</sub> solutions, our eutectic is several degrees higher in temperature than determined by Dobrynina et al. (1980) or Pestova et al. (2005). Our Mg(ClO<sub>4</sub>)<sub>2</sub> solubility data is not consistent with the 216 K eutectic found by Stillman and Grimm (2011) and Toner et al. (2014a). The higher eutectic temperature measured in these studies suggests that a previously uncharacterized, more hydrated Mg(ClO<sub>4</sub>)<sub>2</sub> phase can precipitate from solution during freezing; however, our solubility measurements indicate that Mg(ClO<sub>4</sub>)<sub>2</sub>·6H<sub>2</sub>O does not readily alter to this phase, despite extensive stirring of the solution mixture and long equilibration times (up to several hours) in our measurements.

#### 4.3. Model parameterization to low temperature solubility data

Toner et al. (2015) estimated mixing parameters in the Pitzer model using solubility data; however, there are very few solubility data sets involving perchlorate salts below 298.15 K. If there are no experimental data available for a mixed salt system below 298.15 K, then we assume that the Pitzer parameters determined at 298.15 K by Toner et al. (2015) are constant with temperature. Assuming

temperature-independent parameters is a reasonable approach when experimental data is unavailable because Pitzer parameters change slowly with temperature (Silvester and Pitzer, 1978). Solubilities have been measured in the Na-Cl-ClO<sub>4</sub> system at 293.15 K and 273.15 K (Fig. 6). Following the procedure in Toner et al. (2015), we determined the temperature dependence of the  $\theta_{\text{Cl}^-, \text{ClO}_4^-}$  and  $\psi_{\text{Na}^+, \text{Cl}^-, \text{ClO}_4^-}$  parameters by fitting NaCl and NaClO<sub>4</sub>·H<sub>2</sub>O solubility products to ion activity products modeled in the Na-Cl-ClO<sub>4</sub> system (Table 4). Fig. 6 shows that the solubility of NaCl in the Na-Cl-ClO<sub>4</sub> system is weakly dependent on temperature, whereas the solubility of NaClO<sub>4</sub>·H<sub>2</sub>O decreases by several molal.

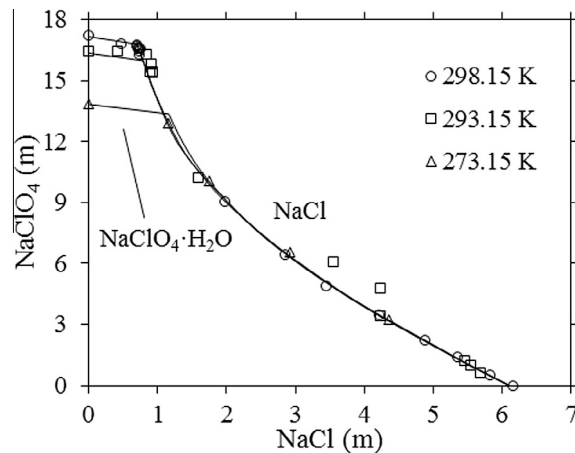


Fig. 6. Experimental data (symbols) from Chan et al. (1995) and modeled (solid lines) solubilities in the Na-Cl-ClO<sub>4</sub> system at 298.15, 293.15, and 273.15 K. The two outlying points at 293.15 K between 3 and 5 m NaCl are not used to fit our model.

## 5. APPLICATION TO THE ROSY RED SOIL SOLUTIONS MEASURED BY THE PHOENIX LANDER

Equilibrium models can be used to estimate what salts may form in soils under various conditions of dehydration and temperature. Marion et al. (2010) studied salts that form from WCL solutions in the presence of ice at low temperatures using FREZCHEM, whereas Toner et al. (2014b) used a chemical divide model. Marion et al. (2010) and Hanley et al. (2012) have also investigated salts that form during evaporation at 280 K, and Toner et al. (2015) has revised FREZCHEM to model evaporation at 298.15 K. The results of these studies indicate that a variety of Ca-Mg carbonate, Mg-Na sulfate, Mg-Na chloride, and Mg-Na-K perchlorate salts precipitate from solution, and that salt assemblages formed during freezing are typically different from salt assemblages formed during evaporation. The accuracy of model predictions in these studies relies upon two key assumptions: (1) liquid water is present to mediate precipitation/dissolution reactions and (2) equilibrium salt assemblages form, as opposed to metastable assemblages. These assumptions are reasonable for the Phoenix site given that there are multiple lines of evidence suggesting liquid water has been active at the Phoenix site (Boynton et al., 2009; Rennó et al., 2009; Smith et al., 2009; Cull et al., 2010; Stillman and Grimm, 2011; Fisher et al., 2014). Furthermore, the ~600 Ma age of the soil (Heet et al., 2009) suggests that there has been sufficient time for brines and salts to equilibrate. Even if liquid water has never formed at the Phoenix site, equilibrium model predictions provide a reference point for interpreting the presence of metastable mineral assemblages (Kounaves et al., 2014b).

### 5.1. Model implementation

We apply our model to ion concentrations in a ‘nominal’ Rosy Red WCL solution from the revised WCL analysis of Toner et al. (2014b):  $\text{Ca}^{2+} = 0.186$ ,  $\text{Mg}^{2+} = 3.459$ ,  $\text{Na}^+ = 1.472$ ,  $\text{K}^+ = 0.329$ ,  $\text{Cl}^- = 0.407$ ,  $\text{SO}_4^{2-} = 1.511$ ,  $\text{ClO}_4^- = 2.743 \text{ mM}$ , Alk. = 2.919 meq, and pH = 7.67. We model *equilibrium* evaporation and/or freezing in contrast to the *fractional* crystallization modeling done by Marion et al. (2010), which assumes that precipitated minerals cannot redissolve into solution. Below 253 K we exclude carbonate chemistries from our model because carbonate equilibria are poorly known below this temperature (Marion, 2001) and because the inclusion of carbonates below 253 K causes convergence failures. The removal of carbonate phases should have a negligible impact on modeled chemistries at lower temperatures given that very little alkalinity remains in solution at 253 K. When carbonates are included in our model (above 253 K), we assume a nominal pCO<sub>2</sub> of 4 mbar in the WCL cell (Kounaves et al., 2010a). We also exclude dolomite ( $\text{CaMg}(\text{CO}_3)_2$ ) and magnesite ( $\text{MgCO}_3$ ) phases from our model because the formation of these salts is kinetically inhibited at low temperatures (Langmuir, 1965; Land, 1998).

To implement our model we use a version of the geochemical program PHREEQC (Appelo and Postma, 2005) developed by Toner and Sletten (2013b) that incorporates Pitzer parameters and solubility products from FREZCHEM in the Na-K-Mg-Ca-H-Cl-SO<sub>4</sub>-OH-HCO<sub>3</sub>-CO<sub>3</sub>-CO<sub>2</sub>-H<sub>2</sub>O system. This version of PHREEQC was tested for freezing seawater and found to be in excellent agreement with FREZCHEM (Fig. 2.2 in Toner and Sletten, 2013a). Our decision to use PHREEQC for our modeling, instead of FREZCHEM, is for a number of reasons: (1) PHREEQC has fewer convergence problems than FREZCHEM, (2) it is much easier to add new phases or parameters to PHREEQC, and (3) many different solutions can be modeled sequentially in PHREEQC. Using the PHREEQC database developed in Toner and Sletten (2013b), we add in additional perchlorate Pitzer parameters and solubility products from this study and from (Toner et al., 2015). We have validated our PHREEQC model by comparing model results to FREZCHEM.

### 5.2. Model results

As a first step, we model freezing of the WCL solution down to its eutectic (Fig. 7). No salts precipitate from solution until below 273.15 K, at which point ice precipitates and concentrates the remaining liquid water. Near 273.15 K, calcite ( $\text{CaCO}_3$ ), hydromagnesite ( $3\text{MgCO}_3 \cdot \text{Mg(OH)}_2 \cdot 3\text{H}_2\text{O}$ ),  $\text{KClO}_4$ , and meridianiite ( $\text{MgSO}_4 \cdot 11\text{H}_2\text{O}$ ) precipitate from solution. At 268.1 K, calcite dissolves into solution and  $\text{Ca}^{2+}$  precipitates as gypsum ( $\text{CaSO}_4 \cdot 2\text{H}_2\text{O}$ ); however, below 261.5 K gypsum dissolves and all  $\text{Ca}^{2+}$  precipitates as calcite. Similarly, mirabilite ( $\text{Na}_2\text{SO}_4 \cdot 10\text{H}_2\text{O}$ ) precipitates at 265.1 K, but redissolves into solution at 253.7 K. The behavior of mirabilite in our model is similar to what occurs in freezing seawater; mirabilite precipitates near 267 K, but redissolves into solution at 251 K (Marion et al., 1999). In seawater, the redissolution of mirabilite has been attributed to the reduction of  $\text{Na}^+$  concentrations due to hydrohalite ( $\text{NaCl} \cdot 2\text{H}_2\text{O}$ ) precipitation. In many experimental studies on freezing seawater, mirabilite persists at lower temperatures due to slow reaction kinetics (e.g. Nelson and Thompson, 1954; Herut et al., 1990); however, more careful experiments with longer equilibration times indicate that mirabilite does dissolve at 251 K (Gitterman, 1937). In our model, mirabilite dissolution at 253.7 K is caused by increasing  $\text{Mg}^{2+}$  ion activity coefficients with increasing perchlorate concentration, leading to greater meridianiite precipitation and lower  $\text{SO}_4^{2-}$  concentrations.

At 234.1 K,  $\text{NaClO}_4 \cdot 2\text{H}_2\text{O}$  precipitates from solution, followed shortly thereafter by  $\text{MgCl}_2 \cdot 12\text{H}_2\text{O}$  at 233.2 K (Fig. 7). Even if  $\text{NaClO}_4$  phases are removed from the model,  $\text{MgCl}_2 \cdot 12\text{H}_2\text{O}$  still precipitates instead of hydrohalite. The precipitation of  $\text{MgCl}_2 \cdot 12\text{H}_2\text{O}$  instead of hydrohalite is surprising because the eutectic temperature of hydrohalite (251.9 K) is significantly higher than  $\text{MgCl}_2 \cdot 12\text{H}_2\text{O}$  (240.2 K) and the solution composition is rich in  $\text{Na}^+$  and  $\text{Cl}^-$  ions at low temperatures. Toner et al. (2014b) also found that  $\text{MgCl}_2 \cdot 12\text{H}_2\text{O}$  precipitates instead of hydrohalite using FREZCHEM, but attributed this

Table 5

Modeled and measured temperatures (Kelvin) and concentrations ( $\text{mol kg}^{-1}$ ) at different phase transitions for  $\text{NaClO}_4$ ,  $\text{Mg}(\text{ClO}_4)_2$ , and  $\text{Ca}(\text{ClO}_4)_2$  salts.

Phase Transition	Modeled	Measured
$\text{NaClO}_4 \cdot \text{H}_2\text{O}-\text{NaClO}_4 \cdot 2\text{H}_2\text{O}$	259.9 K, 12.46 m	259.20 K, 12.44 m <a href="#">Chretien and Kohlmuller (1966)</a>
ice- $\text{NaClO}_4 \cdot 2\text{H}_2\text{O}$	239.2 K, 9.23 m	238.95 K, 9.21 m <a href="#">Chretien and Kohlmuller (1966)</a>
ice- $\text{Ca}(\text{ClO}_4)_2 \cdot 6\text{H}_2\text{O}$	198.2 K, 4.17 m	239.05 K, 9.06 m <a href="#">Hennings et al. (2013)</a>
ice- $\text{Mg}(\text{ClO}_4)_2 \cdot 6\text{H}_2\text{O}$	209.3 K, 3.38 m	212.65 K, 4.62 m <a href="#">Dobrynina et al. (1984)</a>
		198.55 K, 4.20 m <a href="#">Pestova et al. (2005)</a>
		206.15 K, 3.45 m <a href="#">Dobrynina et al. (1980)</a>
		204.55 K, 3.45 m <a href="#">Pestova et al. (2005)</a>

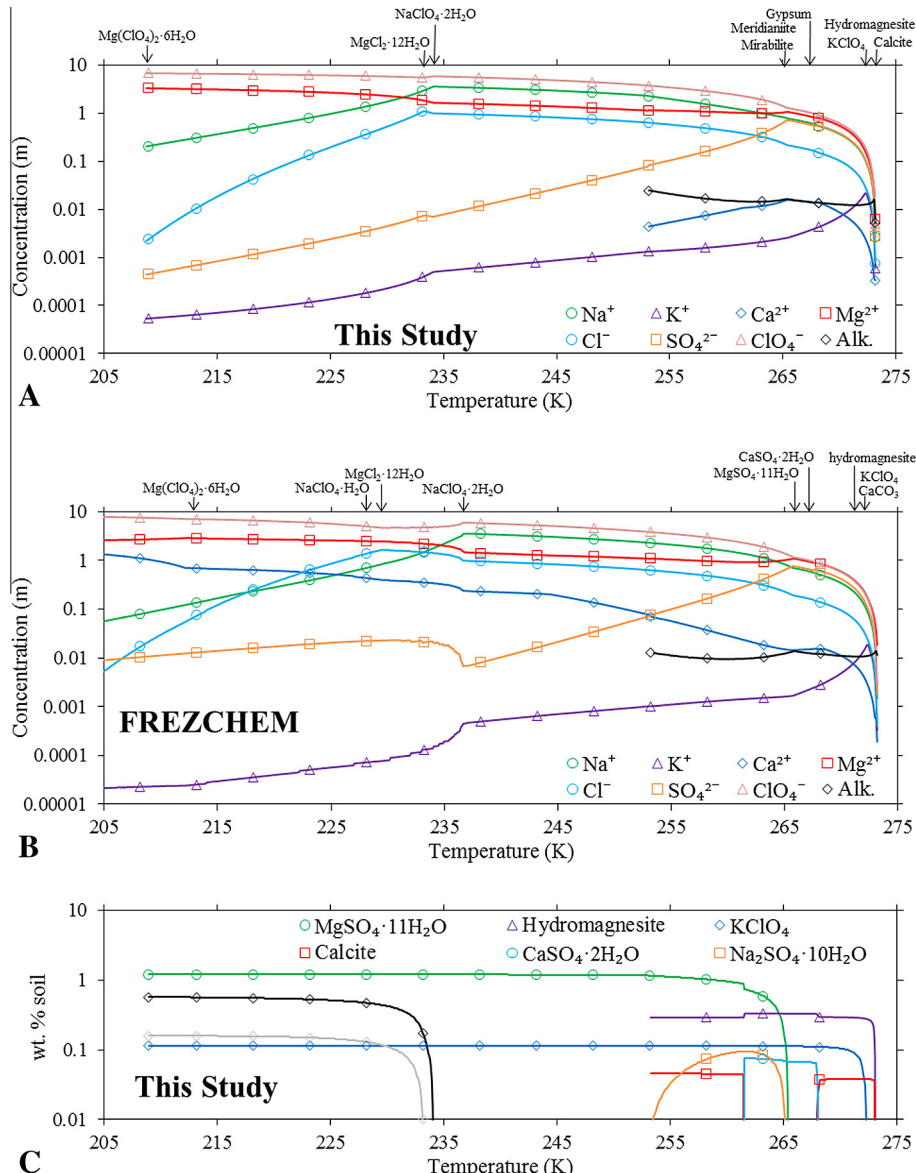


Fig. 7. Modeled freezing of a nominal WCL solution: (A) ion concentrations and salt precipitation events as a function of temperature modeled in this study, (B) ion concentrations and salt precipitation events as a function of temperature modeled with FREZCHEM v.13.3 [Toner et al. \(2014b\)](#). (C) the wt.% of precipitated phases assuming a soil density of  $1 \text{ g cm}^{-3}$  and a total soil addition of 1 g.

apparent reversal in salt solubility to the extremely high  $\text{Mg}^{2+}$  ion activity coefficients that FREZCHEM predicts in perchlorate-rich solutions. As a result, [Toner et al.](#)

(2014b) assumed that hydrohalite precipitates before  $\text{MgCl}_2 \cdot 12\text{H}_2\text{O}$  in their chemical divide model. Although our model predicts much lower  $\text{Mg}^{2+}$  ion activity

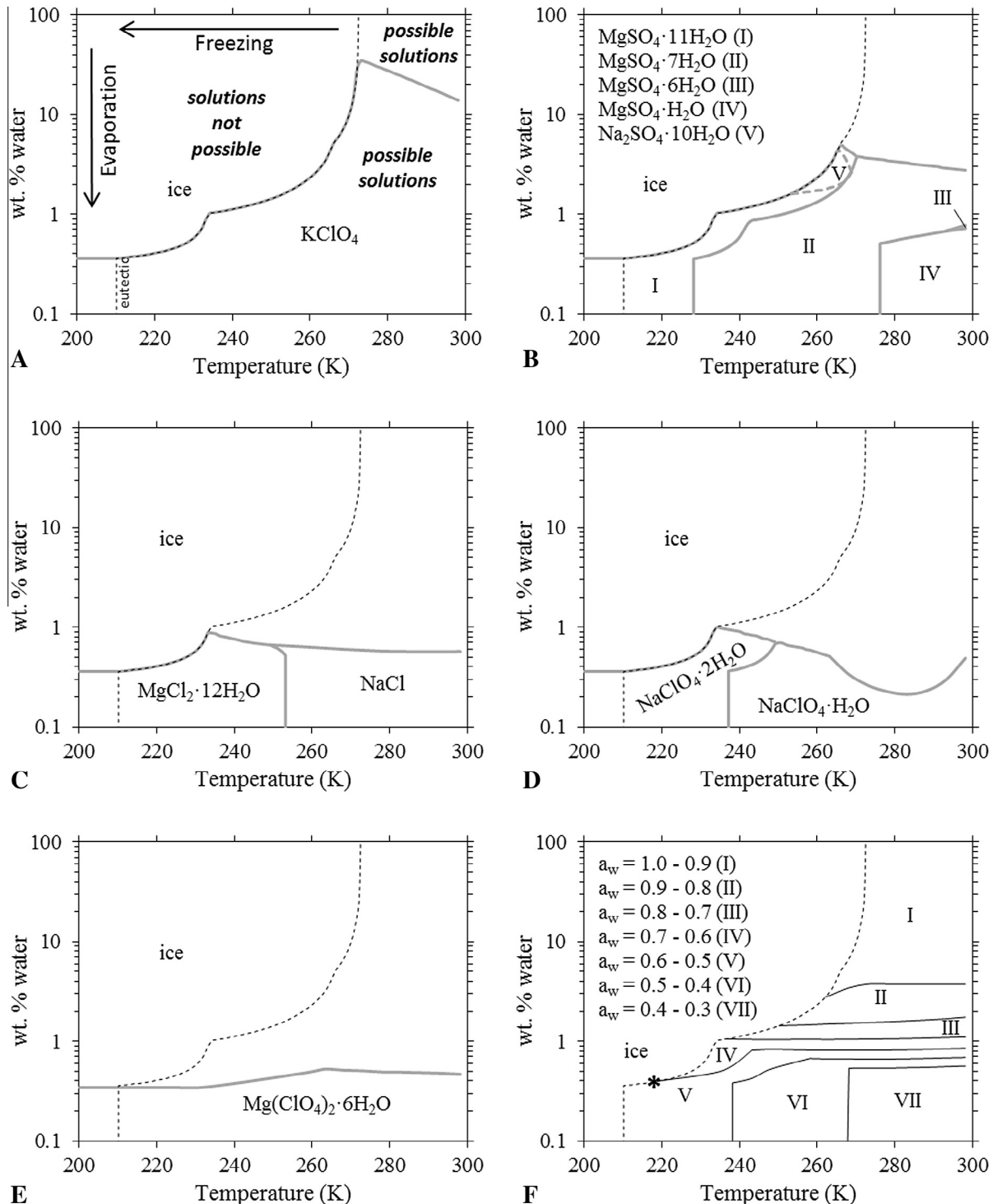


Fig. 8. Modeled stability regions for different solid phases as a function of temperature and residual water content ( $100 \times g_{H_2O} g_{soil}^{-1}$ ) for KClO<sub>4</sub> (A), sulfates (B), chlorides (C), NaClO<sub>4</sub>·2H<sub>2</sub>O/NaClO<sub>4</sub>·H<sub>2</sub>O (D), and Mg(ClO<sub>4</sub>)<sub>2</sub>·6H<sub>2</sub>O (E). Modeled water activities are shown in (F), where the asterisk (\*) indicates the lowest possible temperature where the water activity is 0.6. The dashed lines are the same in all panels and indicate ice precipitation. Soil solutions above the dashed lines cannot occur due to ice precipitation and the resulting decrease in solution water content. The gray lines delineate stability regions for different salts. Note that wt.% water refers to water in solution (i.e. water that would be available to life) and does not include water held in solid phases. To aid in the interpretation of these graphs, panel A has been modified to show the direction of freezing and evaporation, the eutectic, and regions where solutions are possible. As an example, panel A indicates that a solution evaporating at 280 K will precipitate KClO<sub>4</sub> when the liquid water content reaches 27.5 wt.%. Similarly, a freezing WCL solution containing 27.5 wt.% liquid water will precipitate KClO<sub>4</sub> once the temperature decreases to 280 K.

coefficients in perchlorate-rich solutions than FREZCHEM,  $Mg^{2+}$  ion activity coefficients are still much greater than  $Na^+$  ion activity coefficients, leading to an overall ‘salting out’ effect for salts of  $Mg^{2+}$  relative to salts of  $Na^+$ .

The WCL solution finally freezes completely at 209 K when  $Mg(ClO_4)_2 \cdot 6H_2O$  precipitates from a  $Mg(ClO_4)_2$ -rich solution. The total water held in the final salt assemblage is 1.2 wt.% ( $100 \times g_{H_2O} g_{soil}^{-1}$ ), assuming a solution:soil ratio of 25:1  $g_{soil} g_{soil}^{-1}$  in the WCL experiment. As noted by Toner et al. (2014b, 2015), this quantity of water is consistent with measurements of water from orbital spectra (Feldman et al., 2004; Boynton et al., 2007) and *in situ* measurements by the Mars Science Laboratory (MSL) (Leshin et al., 2013; Ming et al., 2013). Furthermore, Toner et al. (2015) found that evaporation at 298.15 K yields hydrated salts with much lower water contents (~0.3 wt.%), suggesting that salts at the Phoenix site, and perhaps elsewhere, formed at low temperatures by freezing. However, the presence of kieserite ( $MgSO_4 \cdot H_2O$ ) (which is inferred to be present on Mars from orbital near-IR spectroscopy) may indicate an evaporative origin in some regions (see below).

Previous studies have modeled either equilibrium freezing starting from a dilute WCL solution, or equilibrium evaporation at a constant temperature; however, these ‘one dimensional’ studies neglect the wide range of dehydration and temperature conditions that are possible in Martian soils. For example, no studies have modeled evaporation at subzero temperatures. Given that Mars’ surface temperature averages ~220 K, evaporation at subzero temperatures may be more relevant to present-day salt assemblages. Whether salts form during evaporation or freezing is dependent on the relative humidity (RH) and temperature. At the soil surface, very low RH conditions occur during the daytime, but RH quickly increases during the nighttime due to lower temperatures (Savijärvi, 1995; Harri et al., 2014). Martín-Torres et al. (2015) found that nighttime relative humidity and soil temperature in Gale Crater, as measured by the Curiosity rover, are high enough to form transient liquid water in the upper 5 cm of soil. Potentially, brines formed during the nighttime could the form salts by evaporation during the daytime; however, Fisher et al. (2014) indicate that hydration/dehydration of brines may be hindered at Mars’ surface temperatures due to slow kinetics. Deeper in the soil, vapor transport is buffered by overlying soil layers and the RH in the soil pore space will be controlled by subsurface ice (Mellon et al., 2009; Smith et al., 2009). Hence, subsurface salts at the Phoenix site likely formed during freezing in equilibrium with ice, which is modeled in Fig. 7.

Starting from an initial dilute WCL solution, we modeled evaporation at different temperatures from 298.15 K down to the WCL solution eutectic at 209 K, and in Fig. 8 we construct the stability regions of different salt precipitates as a function of temperature and wt.% liquid water as grams of water per gram of dry soil ( $100 \times g_{H_2O} g_{soil}^{-1}$ ) (see the Fig. 8 caption for a detailed explanation of how to read these graphs). Due to convergence issues below 253.15 K, we removed alkalinity from the nominal WCL solution

by assuming that alkalinity precipitates entirely as Ca and Mg carbonates. The earliest salt to precipitate from the WCL solution is  $KClO_4$  (Fig 8A).  $KClO_4$  is only completely dissolved above 15–30 wt.% water, which would correspond to a water saturated soil; hence,  $KClO_4$  is likely always present as a precipitated phase. Sulfate salts precipitate in a variety of hydrated phases depending on the temperature and water activity (Fig 8B). In the presence of ice, meridianiite is always the stable  $MgSO_4$  mineral present. Mirabilite also precipitates in the presence of ice, but has a limited stability region between 253 and 269 K. As the WCL solution is further evaporated, meridianiite dehydrates to epsomite ( $MgSO_4 \cdot 7H_2O$ ), hexahydrite ( $MgSO_4 \cdot 6H_2O$ ), and kieserite ( $MgSO_4 \cdot H_2O$ ). Although epsomite and kieserite typically form at higher temperatures, and have been suggested to form on Mars under warm or hot conditions (Noel et al., 2015), our model indicates that epsomite can form down to 228 K and kieserite down to 276 K due to decreasing water activities during evaporation. At low residual water contents, the stability regions of meridianiite, epsomite, and kieserite become constant because all possible salt phases are precipitating from solution, leading to a constant solution composition upon further evaporation. Chloride precipitates entirely as halite ( $NaCl$ ) above 253 K, and then transitions to  $MgCl_2 \cdot 12H_2O$  at lower temperatures (Fig 8C). Although halite transitions to hydrohalite at 273 K in  $NaCl$  solutions, our model indicates that this does not occur in mixture with perchlorate due to lower water activities in concentrated perchlorate solutions and the precipitation of  $MgCl_2 \cdot 12H_2O$ . Similarly, in  $NaClO_4$  solutions,  $NaClO_4 \cdot H_2O$  transitions to  $NaClO_4 \cdot 2H_2O$  at 260 K (Chretien and Kohlmuller, 1966), but the lower water activities in  $NaClO_4 \cdot Mg(ClO_4)_2$  mixtures depresses this transition temperature down to 237 K (Fig 8D).  $Mg(ClO_4)_2 \cdot 6H_2O$  is present in the soil at very advanced states of freezing or evaporation, and only precipitates from solution below 0.5 wt.% water (Fig 8E).

The activity of water in concentrated WCL solutions is critical for the potential habitability of brines and also controls the hydration state of salt precipitates. On Earth,  $a_w = 0.6$  is the lowest known in which life can exist (Grant, 2004; Stevenson et al., 2015). Overall, water activities in our model decrease with water content, and increase with decreasing temperature. At the eutectic temperature of the WCL solution,  $a_w = 0.5–0.6$ . The lowest possible temperature and brine content at which the water activity equals 0.6 is 219 K and 0.4 wt.% water (indicated by the asterisk in Fig 8F). Even higher water activities are possible during daytime temperatures in the summer, which can reach as high as 260 K near the soil surface at the Phoenix site.

## 6. CONCLUSIONS

Salt assemblages on Mars are characteristic of the temperature and relative humidity conditions under which they formed, and reflect the salinity, water activity, and pH of surrounding brines. To predict equilibrium salt assemblages that might occur on Mars, we extended the 298.15 K Pitzer

model of Toner et al. (2015) to lower temperatures using new experimental solubility measurements in perchlorate solutions, including perchlorate mixtures. The resulting model is a significant improvement over FREZCHEM, particularly for mixtures including  $\text{Mg}(\text{ClO}_4)_2$ . Applied to a freezing WCL solution, our model indicates that the WCL solution eutectic is 209 K, and that calcite, hydro-magnesite,  $\text{KClO}_4$ , meridianiite,  $\text{NaClO}_4 \cdot 2\text{H}_2\text{O}$ ,  $\text{MgCl}_2 \cdot 12\text{H}_2\text{O}$ , and  $\text{Mg}(\text{ClO}_4)_2 \cdot 6\text{H}_2\text{O}$  form in order of decreasing temperature. The total water held in hydrated salts at the eutectic is 1.2 wt.% ( $100 \times g_{\text{H}_2\text{O}} g_{\text{soil}}^{-1}$ ), which is consistent with minimum water contents of 1.5–2 wt.% water in Mars' surface soils from *in situ* and orbital measurements, and suggests that salts at the Phoenix site and perhaps elsewhere have formed during freezing.

To determine the full range of salts that might precipitate as a function of temperature and soil water content, we modeled evaporation and freezing of a WCL solution over all possible temperature and soil water content conditions. These comprehensive model results indicate that potentially habitable brines, defined as having a water activity greater than 0.6, only occur above 220 K and 0.4 wt.% water. Overall, the modeling results in this study outline a roadmap of soluble mineral assemblages that are possible under different temperature and soil water content regimes, and can be used to interpret both past and future identifications of soluble minerals on Mars.

#### ACKNOWLEDGEMENTS

Funding from NASA Mars Data Analysis grant #NNX10AN66G awarded to DCC, and from a NASA Astrobiology Institute Postdoc awarded to JDT.

#### REFERENCES

- Appelo C. A. J. and Postma D. (2005) *Geochemistry, Groundwater and Pollution*, second ed. CRC Press, Boca Raton, FL.
- Bandfield J. L., Glotch T. D. and Christensen P. R. (2003) Spectroscopic identification of carbonate minerals in the martian dust. *Science* **301**, 1084–1087.
- Bish D. L., Blake D. F., Vaniman D. T., Chipera S. J., Morris R. V., Ming D. W., Treiman A. H., Sarrazin P., Morrison S. M., Downs R. T., Achilles C. N., Yen A. S., Bristow T. F., Crisp J. A., Morookian J. M., Farmer J. D., Rampe E. B., Stolper E. M., Spanovich N. and Team M. S. (2013) X-ray diffraction results from Mars Science Laboratory: Mineralogy of Rocknest at Gale Crater. *Science* **341**, 1–5.
- Boynton W. V., Ming D. W., Kounaves S. P., Young S. M. M., Arvidson R. E., Hecht M. H., Hoffman J., Niles P. B., Hamara D. K., Quinn R. C., Smith P. H., Sutter B., Catling D. C. and Morris R. V. (2009) Evidence for calcium carbonate at the Mars Phoenix landing site. *Science* **325**, 61–64.
- Boynton W. V., Taylor G. J., Evans L. G., Reedy R. C., Starr R., Janes D. M., Kerr K. E., Drake D. M., Kim K. J., Williams R. M. S., Crombie M. K., Dohm J. M., Baker V., Metzger A. E., Karunatillake S., Keller J. M., Newsom H. E., Arnold J. R., Bruckner J., Englert P. A. J., Gasnault O., Sprague A. L., Mitrofanov I., Squyres S. W., Trombka J. I., d'Uston L., Wanke H. and Hamara D. K. (2007) Concentration of H, Si, Cl, K, Fe, and Th in the low- and mid-latitude regions of Mars. *J. Geophys. Res.* **112**, 1–15.
- Chan C., Khoo K. H., Gryzlova E. S. and Adad M. (1995) *Alkali metal and ammonium perchlorates: part 1: lithium and sodium perchlorates*. Oxford University Press.
- Chan, C., Lepeshkov, I. N., HKhoo and K. H. (1989) Alkaline earth metal perchlorates. Permagon Press.
- Chretien A. and Kohlmuller R. (1966) Perchlorate de sodium. In *Nouveau Traité de Chimie Minerale, Sodium and Lithium* (ed. P. Pascal). Masson & Cie, Paris, pp. 344–354.
- Cull S., Kennedy E. and Clark A. (2014) Aqueous and non-aqueous soil processes on the northern plains of Mars: insights from the distribution of perchlorate salts at the Phoenix landing site and in Earth analog environments. *Planet. Space Sci.* **96**, 29–34.
- Cull S. C., Arvidson R. E., Catalano J. G., Ming D. W., Morris R. V., Mellon M. T. and Lemmon M. (2010) Concentrated perchlorate at the Mars Phoenix landing site: evidence for thin film liquid water on Mars. *Geophys. Res. Lett.* **37**, 1–6.
- Dobrynina T. A., Akhapkina N. A. and Rosolovskii V. Y. (1984) The fusion diagram of the calcium perchlorate-water system. *Russ. J. Inorg. Chem.* **29**, 1043–1045.
- Dobrynina T. A., Chernyshova A. M., Akhapkina N. A. and Rosolovskii V. Y. (1980) Fusion diagram of the magnesium perchlorate-water system. *Russ. J. Inorg. Chem.* **25**, 2233–2236.
- Ehlmann B. L., Mustard J. F., Murchie S. L., Poulet F., Bishop J. L., Brown A. J., Calvin W. M., Clark R. N., Des Marais D. J., Milliken R. E., Roach L. H., Roush T. L., Swayze G. A. and Wray J. J. (2008) Orbital identification of carbonate-bearing rocks on Mars. *Science* **322**, 1828–1832.
- Feldman W. C., Prettyman T. H., Maurice S., Plaut J. J., Bish D. L., Vaniman D. T., Mellon M. T., Metzger A. E., Squyres S. W., Karunatillake S., Boynton W. V., Elphic R. C., Funsten H. O., Lawrence D. J. and Tokar R. L. (2004) Global distribution of near-surface hydrogen on Mars. *J. Geophys. Res.* **109**, 1–13.
- Fisher E., Martinez G. M., Elliot H. M. and Rennó N. O. (2014) Experimental evidence for the formation of liquid saline water on Mars. *Geophys. Res. Lett.* **41**, 4456–4462.
- Freeth F. A. (1924) Ternary and quaternary equilibria in the system:  $\text{NaClO}_4 \cdot (\text{NH}_4)_2\text{SO}_4 \cdot \text{NH}_4\text{ClO}_4 \cdot \text{Na}_2\text{SO}_4 \cdot \text{H}_2\text{O}$ , at 60° and 25 °C. *Recl. Trav. Chim. Pays-Bas* **43**, 475–507.
- Gendrin A., Mangold N., Bibring J. P., Langevin Y., Gondet B., Poulet F., Bonello G., Quantin C., Mustard J. F. and Arvidson R. (2005) Sulfates in Martian Layered Terrains: The OMEGA/Mars Express View. *Science* **307**, 1587–1591.
- Gier L. J. and Vanderzee C. E. (1974) Enthalpies of dilution and relative apparent molar enthalpies of aqueous calcium and manganese perchlorates. *J. Chem. Eng. Data* **19**, 323–325.
- Gitterman, K. E. (1937) Thermal analysis of sea water, In (ed. C. TL). USA Cold Regions Research and Engineering Laboratory, Hanover, NH.
- Grant W. D. (2004) Life at low water activity. *Philos. Trans. R. Soc. London: Biol. Sci.* **359**, 1249–1267.
- Hanley J., Chevrier V. F., Berget D. J. and Adams R. D. (2012) Chlorate salts and solutions on Mars. *Geophys. Res. Lett.* **39**, 1–5.
- Harri A. M., Genzer M., Kemppinen O., Gomex-Elvira J., Haberle R. M., Polkko J., Savijärvi H., Rennó N., Rodriguez-Manfredi J. A., Schmidt W., Richardson M., Siili T., Paton M., De La Torre-Juarez M., Mäkinen T., Newman C., Rafkin S., Mischna M., Merikallio S., Haukka H., Martin-Torres J., Komu M., Zorzano M. P., Peinado V., Vazquez L. and Urqui R. (2014) Mars science laboratory relative humidity observations – initial results. *J. Geophys. Res.* **119**, 2132–2147.
- Harvie C. E. and Weare J. H. (1980) The prediction of mineral solubilities in natural waters: the Na-K-Mg-Ca-Cl-SO<sub>4</sub>-H<sub>2</sub>O system from zero to high concentration at 25 °C. *Geochim. Cosmochim. Acta* **44**, 981–997.

- Hecht M. H., Kounaves S. P., Quinn R. C., West S. J., Young M. M., Ming D. W., Catling D. C., Clark B. C., Boynton W. V., Hoffman J., DeFlores L. P., Gospodinova K., Kapit J. and Smith P. H. (2009) Detection of perchlorate and the soluble chemistry of martian soil at the Phoenix Lander Site. *Science* **325**, 64–67.
- Heet T. L., Arvidson R. E., Cull S. C., Mellon M. T. and Seelos K. D. (2009) Geomorphic and geologic settings of the Phoenix Lander mission landing site. *J. Geophys. Res. Planet.* **114**, 1–19.
- Hennings E., Schmidt H. and Voigt W. (2014) Crystal structures of  $\text{Ca}(\text{ClO}_4)_2 \cdot 4\text{H}_2\text{O}$  and  $\text{Ca}(\text{ClO}_4)_2 \cdot 6\text{H}_2\text{O}$ . *Acta Crystallograph. Sec. E: Struct. Rep.* **E70**, 489–493.
- Hennings E., Zürner P., Schmidt H., Voigt W., Heinz J., Schmidt H. and Voigt W. (2013) Freezing and hydrate formation in aqueous sodium perchlorate solutions. *Zeitschrift für anorganische und allgemeine Chemie* **639**, 922–927.
- Herut B., Starinsky A., Katz A. and Bein A. (1990) The role of seawater freezing in the formation of subsurface brines. *Geochim. Cosmochim. Acta* **54**, 13–21.
- Jongenburger H. S. and Wood R. H. (1965) The heats and entropies of dilution of the perchlorates of magnesium and strontium. *J. Phys. Chem.* **69**, 4231–4238.
- Kounaves S. P., Carrera G. D., O'Neil G. D., Stroble S. T. and Claire M. W. (2014a) Evidence of martian perchlorate, chloride, and nitrate in Mars meteorite EETA79001: implications for oxidants and organics. *Icarus* **229**, 206–213.
- Kounaves S. P., Chaniotakis N. A., Chevrier V. F., Carrier B. L., Folds K. E., Hansen V. M., McElhoney K. M., O'Neil G. D. and Weber A. W. (2014b) Identification of the perchlorate parent salts at the Phoenix Mars landing site and possible implications. *Icarus* **232**, 226–231.
- Kounaves S. P., Hecht M. H., Kapit J., Gospodinova K., DeFlores L., Quinn R. C., Boynton W. V., Clark B. C., Catling D. C., Hredzak P., Ming D. W., Moore Q., Shusterman J., Stroble S., West S. J. and Young S. M. M. (2010a) Wet chemistry experiments on the 2007 Phoenix Mars Scout Lander mission: data analysis and results. *J. Geophys. Res.* **115**, 1–16.
- Kounaves S. P., Hecht M. H., Kapit J., Quinn R. C., Catling D. C., Clark B. C., Ming D. W., Gospodinova K., Hredzak P., McElhoney K. and Shusterman J. (2010b) Soluble sulfate in the martian soil at the Phoenix landing site. *Geophys. Res. Lett.* **37**, 1–5.
- Kounaves S. P., Stroble S. T., Anderson R. M., Moore Q., Catling D. C., Douglas S., McKay C. P., Ming D. W., Smith P. H., Tamppari L. K. and Zent A. P. (2010c) Discovery of natural perchlorate in the Antarctic Dry Valleys and its global implications. *Environ. Sci. Technol.* **44**, 2360–2364.
- Land L. S. (1998) Failure to precipitate dolomite at 25 °C from dilute solution despite 1000-fold oversaturation after 32 years. *Aquat. Geochem.* **4**, 361–368.
- Langevin Y., Poulet F., Bibring J. P. and Gondet B. (2005) Sulfates in the north polar region of Mars detected by OMEGA/Mars express. *Science* **307**, 1584–1586.
- Langmuir D. (1965) Stability of carbonates in the system  $\text{MgO}-\text{CO}_2\text{-H}_2\text{O}$ . *J. Geol.* **73**, 730–754.
- Leshin L. A., Mahaffy P. R., Webster C. R., Cabane M., Coll P., Conrad P. G., Archer P. D., Atreya S. K., Brunner A. E., Buch A., Eigenbrode J. L., Flesch G. J., Franz H. B., Freissinet C., Glavin D. P., McAdam A. C., Miller K. E., Ming D. W., Morris R. V., Navarro-González R., Niles P. B., Owen T., Pepin R. O., Squyres S. W., Steel A., Stern J. C., Summons R. E., Sumner D. Y., Sutter B., Szopa C., Teinturier S., Trainer M. G., Wray J. J., Grotzinger J. P. and Team M. S. (2013) Volatile, isotope, and organic analysis of martian fines with the mars curiosity rover. *Science* **341**, 1–9.
- Marion G. M. (2001) Carbonate mineral solubility at low temperatures in the  $\text{Na-K-Mg-Ca-H-Cl-SO}_4\text{-OH-HCO}_3\text{-CO}_3\text{-CO}_2\text{-H}_2\text{O}$  system. *Geochim. Cosmochim. Acta* **65**, 1883–1896.
- Marion G. M., Catling D. C., Zahnle K. J. and Claire M. W. (2010) Modeling aqueous perchlorate chemistries with applications to Mars. *Icarus* **207**, 675–685.
- Marion G. M., Farren R. E. and Komrowski A. J. (1999) Alternative pathways for seawater freezing. *Cold Reg. Sci. Technol.* **29**, 259–266.
- Marion G. M. and Kargel J. S. (2008) *Cold Aqueous Planetary Geochemistry with FREZCHEM: From Modeling to the Search for Life at the Limits*. Springer, Berlin/Heidelberg.
- Martín-Torres F. J., Zorzano M. P., Valentín-Serrano P., Harri A. M., Genzer M., Kemppinen O., Rivera-Valentin E. G., Jun I., Wray J. J., Madsen M. B., Goetz W., McEwen A. S., Hardgrove C., Renno N., Chevrier V. F., Mischna M., Navarro-González R., Martínez-Frías J., Conrad P. G., McConnochie T., Cockell C. S., Berger G., Vasadada A. R., Sumner D. and Vaniman D. T. (2015) Transient liquid water and water activity at Gale crater on Mars. *Nat. Geosci.* **8**, 357–361.
- Mellan M. T., Arvidson R. E., Sizemore H. G., Searls M. L., Blaney D. L., Cull S., Hecht M. H., Heet T. L., Keller H. U., Lemmon M. T., Markiewicz W. J., Ming D. W., Morris R. V., Pike W. T. and Zent A. P. (2009) Ground ice at the Phoenix Landing Site: stability state and origin. *J. Geophys. Res.* **114**, 1–15.
- Ming D. W., Archer P. D., Glavin D. P., Eigenbrode J. L., Franz H. B., Sutter B., Brunner A. E., Stern J. C., Freissinet C., McAdam A. C., Mahaffy P. R., Cabane M., Coll P., Campbell J. L., Atreya S. K., Niles P. B., Bell J. F., Bish D. L., Brinckerhoff W. B., Buch A., Conrad P. G., Des Marais D. J., Ehlmann B. L., Fairén A. G., Farley K., Flesch G. J., Francois P., Gellert R., Grant J. A., Grotzinger J. P., Gupta S., Herkenhoff K. E., Hurowitz J. A., Leshin L. A., Lewis K. W., McLennan S. M., Miller K. E., Moersch J., Morris R. V., Navarro-González R., Pavlov A. A., Perrett G. M., Pradler I., Squyres S. W., Summons R. E., Steele A., Stolper E. M., Sumner D. Y., Szopa C., Teinturier S., Trainer M. G., Treiman A. H., Vaniman D. T., Vasavada A. R., Webster C. R., Wray J. J. and Yingst R. A. (2013) Volatile and organic compositions of sedimentary rocks in Yellowknife Bay, Gale Crater, Mars. *Science* **343**, 1–9.
- Morris R. V., Ruff S. W., Gellert R., Ming D. W., Arvidson R. E., Clark B. C., Golden D. C., Siebach K., Klingelhofer G., Schroder C., Fleischer I., Yen A. S. and Squyres S. W. (2010) Identification of carbonate-rich outcrops on Mars by the Spirit Rover. *Science* **329**, 421–424.
- Murchie S. L., Mustard J. F., Ehlmann B. L., Milliken R. E., Bishop J. L., McKeown N. K., Dobrea E. Z. N., Seelos F. P., Buczkowski D. L., Wiseman S. M., Arvidson R. E., Wray J. J., Swayze G., Clark R. N., Marais D. J. D., McEwen A. S. and Bibring J. P. (2009) A synthesis of Martian aqueous mineralogy after 1 Mars year of observations from the Mars Reconnaissance Orbiter. *J. Geophys. Res.* **114**, 1–30.
- Navarro-González R., Vargas E., de la Rosa J., Raga A. and McKay C. (2010) Reanalysis of the Viking results suggests perchlorate and organics at midlatitudes on Mars. *J. Geophys. Res. Planet.* **115**, 1–11.
- Nelson K. H. and Thompson T. G. (1954) *Deposition of salts from sea water by frigid concentration*. University of Washington Dept. of Oceanography, Seattle, WA.
- Nicholson D. E. and Felsing W. A. (1950) The determination of the activity coefficients of the alkaline earth and magnesium perchlorates from freezing point data. *J. Am. Chem. Soc.* **72**, 4469–4471.

- Niles P. B., Catling D. C., Berger G., Chassefière E., Ehmann B. L., Michalski J. R., Morris R. V., Ruff S. W. and Sutter B. (2013) Geochemistry of carbonates on mars: implications for climate history and nature of aqueous environments. *Space Sci. Rev.* **174**, 301–328.
- Noel A., Bishop J. L., Al-Samir M., Gross C., Flahaut J., McGuire P. C., Weitz C. M., Seelos F. P. and Murchie S. L. (2015) Mineralogy, morphology and stratigraphy of the light-toned interior layered deposits at Juventae Chasma. *Icarus* **251**, 315–331.
- Osterloo M. M., Hamilton V. E., Bandfield J. L., Glotch T. D., Baldridge A. M., Christensen P. R., Tornabene L. L. and Anderson F. S. (2008) Chloride-bearing materials in the southern highlands of Mars. *Science* **319**, 1651–1654.
- Pátek J., Klomfar J. and Součková M. (2008) Solid–Liquid equilibrium in the system of  $\text{CaCl}_2\text{-H}_2\text{O}$  with special regard to the transition points. *J. Chem. Eng. Data* **53**, 2260–2271.
- Pestova O. N., Myund L. A., Khrapun M. K. and Prigaro A. V. (2005) Polythermal study of the systems  $\text{M}(\text{ClO}_4)_2\text{-H}_2\text{O}$  ( $\text{M}^{2+} = \text{Mg}^{2+}, \text{Ca}^{2+}, \text{Sr}^{2+}, \text{Ba}^{2+}$ ). *Russ. J. Appl. Chem.* **78**, 409–413.
- Pitzer K. S. (1991) *Ion interaction approach: theory and data correlation, activity coefficients in electrolyte solutions*, second ed. CRC Press, Boca Raton, pp. 75–153.
- Rennó N. O., Bos B. J., Catling D. C., Clark B. C., Drube L., Fisher D., Goetz W., Hviid S. F., Keller H. U., Kok J. F., Kounaves S. P., Leer K., Lemmon M. T., Madsen M. B., Markiewicz W. J., Marshall J., McKay C., Mehta M., Smith M., Zorzano M. P., Smith P. H., Stoker C. and Young S. M. M. (2009) Possible physical and thermodynamical evidence for liquid water at the Phoenix landing site. *J. Geophys. Res.* **114**, 1–11.
- Robinson R. A. and Stokes R. H. (1959) *Electrolyte Solutions*, second ed. Butterworths, London.
- Ruesch O., Poulet F., Vincendon M., Bibring J. P., Carter J., Erkeling G., Gondet B., Hiesinger H., Ody A. and Reiss D. (2012) Compositional investigation of the proposed chloride-bearing materials on Mars using near-infrared orbital data from OMEGA/MEx. *J. Geophys. Res.* **117**, 1–18.
- Savijärvi H. (1995) Mars boundary layer modeling: diurnal moisture cycle and soil properties at the viking lander 1 site. *Icarus* **117**, 120–127.
- Scatchard G., Jones P. T. and Prentiss S. S. (1932) The freezing points of aqueous solutions. I. A freezing point apparatus. *J. Am. Chem. Soc.* **54**, 2676–2690.
- Scatchard G., Prentiss S. S. and Jones P. T. (1934) The freezing points of aqueous solutions. V. Potassium, sodium and lithium chlorates and perchlorates. *J. Am. Chem. Soc.* **56**, 805–807.
- Silvester L. F. and Pitzer K. S. (1978) Thermodynamics of electrolytes. X. Enthalpy and the effect of temperature on the activity coefficients. *J. Solution Chem.* **7**, 327–337.
- Smith P. H., Tamppari L. K., Arvidson R. E., Bass D., Blaney D., Boynton W. V., Carswell A., Catling D. C., Clark B. C., Duck T., DeJong E., Fisher D., Goetz W., Gunnlaugsson H. P., Hecht S. P., Hipkin V., Hoffman J., Hviid S. F., Keller H. U., Kounaves S. P., Lange C. F., Lemmon M. T., Madsen M. B., Markiewicz W. J., Marshall J., McKay C. P., Mellon M. T., Ming D. W., Morris R. V., Pike W. T., Renno N., Staufer U., Stoker C., Taylor P., Whiteway J. A. and Zent A. P. (2009)  $\text{H}_2\text{O}$  at the Phoenix Landing Site. *Science* **325**, 58–61.
- Spencer R. J., Møller N. and Weare J. H. (1990) The prediction of mineral solubilities in natural waters: a chemical equilibrium model for the  $\text{Na-K-Ca-Mg-Cl-SO}_4\text{-H}_2\text{O}$  system at temperatures below 25°C. *Geochim. Cosmochim. Acta* **54**, 575–590.
- Stevenson A., Burkhardt J., Cockell C. S., Cray J. A., Dijksterhuis J., Fox-Powell M., Kee T. P., Kminek G., McGinity T. J., Timmis K. N., Timson D. J., Voytek M. A., Westall F., Yakimov M. M. and Hallsworth J. E. (2015) Multiplication of microbes below 0.690 water activity: implications for terrestrial and extraterrestrial life. *Environ. Microbiol.* **17**, 257–277.
- Stillman D. E. and Grimm R. E. (2011) Dielectric signatures of adsorbed and salty liquid water at the Phoenix landing site, Mars. *J. Geophys. Res.* **116**, 1–11.
- Toner J. D., Catling D. C. and Light B. (2014a) The formation of supercooled brines, viscous liquids, and low temperature perchlorate glasses in aqueous solutions relevant to Mars. *Icarus* **233**, 36–47.
- Toner J. D., Catling D. C. and Light B. (2014b) Soluble salts at the Phoenix Lander site, Mars: A reanalysis of the Wet Chemistry Laboratory data. *Geochim. Cosmochim. Acta* **136**, 142–168.
- Toner J. D., Catling D. C. and Light B. (2015) Modeling salt precipitation from brines on Mars: evaporation versus freezing origin for soil salts. *Icarus* **250**, 451–461.
- Toner J. D. and Sletten R. S. (2013a) The formation of Ca-Cl-rich groundwaters in the Dry Valleys of Antarctica: field measurements and modeling of reactive transport. *Geochim. Cosmochim. Acta* **110**, 84–105.
- Toner J. D. and Sletten R. S. (2013b) The formation of Ca-Cl enriched groundwaters in the Dry Valleys of Antarctica by cation exchange reactions: field measurements and modeling of reactive transport. *Geochim. Cosmochim. Acta* **110**, 84–105.
- Vanderzee C. E. and Swanson J. A. (1963) Heats of dilution and relative apparent molal enthalpies of aqueous sodium perchlorate and perchloric acid. *J. Phys. Chem.* **67**, 285–291.
- Yen A. S., Gellert R., Schröder C., Morris R. V., Bell J. F., Knudson A. T., Clark B. C., Ming D. W., Crisp J. A., Arvidson R. E., Blaney D., Brückner J., Christensen P. R., DesMarais D. J., Souza P. A., Economou T. E., Ghosh A., Hahn B. C., Kerkenhoff K. E., Haskin L. A., Hurowitz J. A., Joliff B. L., Johnson J. R., Klingelhöfer G., Madsen M. B., McLennan S. M., McSween H. Y., Richter L., Rieder R., Rodionov D., Soderblom L., Squyres S. W., Tosca N. J., Wang A., YWyatt M. and Zipfel J. (2005) An integrated view of the chemistry and mineralogy of martian soils. *Nature* **436**, 49–54.

Associate editor: Jeffrey G. Catalano